Ref.: GEB-2017-0193,R1

Dear editors,

Thank you for the great news, we are so pleased to publish in this journal. We have provided answers to editor's checklist in context. Our answers appear in a difference font and color: **Response to checklist**. The paper revision returned is the last version submitted with track changes left on reflecting the minor changes below, now called: Friedland global blooms 07a.docx.

Sincerely, Kevin Friedland

09-Dec-2017

Dear Dr. Friedland

Re: 'Phenology and time series trends of the dominant seasonal phytoplankton bloom across global scales' (Ref. GEB-2017-0193.R1).

Congratulations. We are pleased to accept the above article for publication
in Global Ecology and Biogeography!

Your paper will now be sent to Wiley for copy editing and typesetting and we will contact you if there are any queries.

Thank you for helping to make Global Ecology and Biogeography such a great journal.

Yours sincerely,
Brian McGill, Maria Dornelas and Richard Field
Editors-in-Chief, Global Ecology and Biogeography

EDITOR-IN-CHIEF'S COMMENTS TO AUTHORS

EDITOR'S COMMENTS TO AUTHORS
Editor: Leprieur, Fabien
Comments to the Author:
(There are no comments.)

Dr. Fabien Leprieur, Editor

To ensure that your paper goes into production smoothly, please check the following:
1. A biosketch and a data availability statement should be included.

Biosketch is provided, data availability expanded to include the Ocean Data Assimilation Experiment data.

2. A short running header should be included to go at the top of the journal page.
Running head added.

3. Citations in the text should be in house style.
Citations are in EndNote using the Global Ecology and Biogeography style definition.

4. English spellings should be used throughout the text.
English spelling used.

5. The reference list should be in house style.
Reference list is in EndNote using the Global Ecology and Biogeography style definition.

6. All the citations in the text should be listed in the References.
Done.

7. The figures and tables should be in numerical order.
Figures are in numerical order.

8. High quality figures are ready to be supplied (see below).
Figures done as 300dpi PNG files.

9. Please note that any supplementary material will not be copy-edited and so should be supplied in its final state.
Supplementary material is in final form.

10. A short title (not a complete legend) should be supplied for each numbered item in the supplementary material. These will be printed near the end of the article.
Added to material.

11. Colour figures:
a) By default, all of your figures will appear in colour online but in black-and-white for the limited print circulation. Therefore, these figures must be understandable in both the colour and black andwhite versions.

b) If you wish any figures to appear in color in the print version, there is a charge to print the colour figures. For these figures, please complete the payment process via Wiley's Author Services system. You will receive an email about this.
Default accepted.

12. High quality figures
We will require separate high quality versions of each figure, if you have not already provided them. High resolution figure files should be submitted to the production editor at GEB@wiley.com only after first proof is ready, together with answers to author queries raised for your manuscript. Please make sure you have named them appropriately (e.g. GEB-2012-0124-Fig1.tif). You will be contacted by the Production Editor if there are any problems with the resolution and/or format of any figures.

Photographic figures should be supplied in tif format (or jpg format with low compression). These should be at 300 d.p.i. after sizing. Line figures and combination figures should preferentially be supplied as vector graphics (not pixel-based graphics) in pdf or eps format (or as vector graphics embedded into a Word document). Failing that, high-resolutions tif (not jpg) versions of line/combination figures may be supplied (but note that online publication quality will not be as good as with vector formats). Further instructions on the preparation of figures and acceptable file formats are provided in Author Guidelines on the journal homepage (http://onlinelibrary.wiley.com/journal/10.1111/(ISSN)1466-8238).

Figures done as 300dpi PNG files.

13. Publication options and licencing agreements
Your article cannot be published until you have signed the appropriate licence agreement. Within the next few days you will receive an email from Wiley's Author Services system which will ask you to log in and will present you with the appropriate licence for completion.

There are two options for publication in Global Ecology and Biogeography, which are described in the following sections a) and b).

a) If you choose the publication option whereby your article will be in the hard-copy journal, and accessible on-line to subscribers to Global Ecology and Biogeography, the only cost to the author is for the printing of the colour images (i.e., those listed in 11b above, if any).

b) OnlineOpen
The second option for publication is Online Open, where in addition to appearing in the hard copy journal, the online version on Wiley Online Library will be open access, i.e. free for all to view anddownload.

OnlineOpen is available to authors of articles who wish to make their article open access. With OnlineOpen the author, their funding agency, or institution pays a fee to ensure that the article is made available to non-subscribers upon publication via Wiley Online Library, as well as deposited in PubMed Central and PMC mirror sites. In addition to publication online via Wiley Online Library, authors of OnlineOpen articles are permitted to post the final, published PDF of their article on a website, institutional repository, or other free public server, immediately on publication.

If you want your article to be open access please choose the appropriate licence agreement when you log in to Wiley's Author Services system. click on 'Make my article OnlineOpen' and choose the appropriate license by clicking on 'Sign license agreement now' when you log in to Wiley's Author Services system. This option has a charge, which is additional to any charge for colour figures that may apply to the article. See 'Author Guidelines' on the Global Ecology and Biogeography web site (http://wileyonlinelibrary.com) for journal-specific instructions, andhttp://wileyonlinelibrary.com/onlineopen#OnlineOpen_Terms for general information about Online Open.
Publication option.

14. Production status tracking
You can now track your article via the publisher's Author Services. Once your paper is with the Production Editor, you will receive an e-mail with a unique code that automatically adds your article to the system when you register. With Author Services you can check the status of your article online and choose to receive automated e-mails at key stages of production.
Understood

15. Proof stage
Global Ecology and Biogeography uses an "e-proofing" service. You will receive an e-mail from the typesetter when your article is ready for proofing, providing instructions about how to download and return your proof. In the meantime, should you change your default email address, please ensure that you send us your updated details.
Understood

16. Offprints
The corresponding author automatically receives a free PDF offprint by e-mail upon print publication of the article, along with full terms and conditions of use. Printed offprints can be ordered anddetails of ordering and costs will be sent along with the first proof to the corresponding author.
Understood

17. Cover image

If you would like images from your paper, or an alternative image related to the work, to be considered for the cover, please email your layout suggestions to covers@wiley.com. While we typically ask authors to contribute toward the production cost of cover illustrations, we are currently waiving that amount. Please see our Cover FAQ at http://olabout.wiley.com/WileyCDA/Section/id-827445.html for details on cover image preparation.

No cover image supplied.

Phenology and time series trends of the dominant seasonal phytoplankton bloom across global scales

Kevin D. Friedland[1,*], Colleen B. Mouw[2], Rebecca G. Asch[3,4], A. Sofia A. Ferreira[5], Stephanie Henson[6], Kimberly J. W. Hyde[1], Ryan E. Morse[1], Andrew C. Thomas[7], Damian C. Brady[7]

[1]National Marine Fisheries Service, 28 Tarzwell Dr., Narragansett, RI 02882, USA
[2]University of Rhode Island, Graduate School of Oceanography, 215 South Ferry Road, Narragansett, RI 02882, USA
[3] Princeton University, Program in Atmospheric and Oceanic Sciences, 300 Forrestal Road, Princeton, NJ 08540, USA
[4] Current address: East Carolina University, Department of Biology, 1000 East 5th Street, Greenville, NC 27858, USA
[5]School of Oceanography, University of Washington, Seattle, WA, USA
[6]National Oceanography Centre, European Way, Southampton, UK
[7]School of Marine Sciences, University of Maine, Orono, ME, USA

Kevin D. Friedland (kevin.friedland@noaa.gov)
Colleen B. Mouw (cmouw@uri.edu)
Rebecca G. Asch (aschr16@ecu.edu)
A. Sofia A. Ferreira (asofiaaferreira@gmail.com)
Stephanie Henson (S.Henson@noc.ac.uk)
Kimberly J. W. Hyde (kimberly.hyde@noaa.gov)
Ryan E. Morse (ryan.morse@noaa.gov)
Andrew C. Thomas (thomas@maine.edu)
Damian C. Brady (damian.brady@maine.edu)

Keywords: phytoplankton, bloom, phenology, trend analysis, carbon cycle, productivity

*Correspondence: Kevin Friedland, National Marine Fisheries Service, 28 Tarzwell Dr., Narragansett, RI 02882, USA, E-mail: kevin.friedland@noaa.gov

Number of words in the Abstract: 291

Number of words in main body of the paper: 8396

Number of references: 87

Running head: Global Bloom Phenology

ABSTRACT

Aim This study examined phytoplankton blooms on a global scale with the intention of describing patterns of bloom timing and size, the effect of bloom timing on the size of blooms, and time series trends in bloom characteristics.

Location Global.

Methods We used a change-point statistics algorithm to detect phytoplankton blooms in time series of chlorophyll concentration data over a global grid. At each study location, the bloom statistics for the dominant bloom, based on the search time period that resulted in the most blooms detected, were used to describe the spatial distribution of bloom characteristics over the globe. Time series of bloom characteristics were also subjected to trend analysis to describe regional and global change in bloom timing and size.

Results The characteristics of the dominant bloom were found to vary with latitude and in localized patterns associated with specific oceanographic features. Bloom timing had the most profound effect on bloom duration, with early blooms tending to last longer than later starting blooms. Time series of bloom timing and duration were trended, suggesting blooms have been starting earlier and lasting longer, respectively, on a global scale. Blooms have also increased in size at high latitudes and decreased in equatorial areas based on multiple size metrics.

Main conclusions Phytoplankton blooms have changed on both regional and global scales, which has ramifications for the function of food webs providing ecosystem services. A tendency for blooms to start earlier and last longer will have an impact on energy flow pathways in ecosystems, differentially favoring the productivity of different species groups. These changes may also affect the sequestration of carbon in ocean ecosystems. A shift to earlier bloom timing is consistent with the expected effect of warming ocean climate conditions observed in recent decades.

INTRODUCTION

Primary production in the oceans accounts for approximately half of the carbon fixed by photosynthesis on a global scale (Field *et al.*, 1998). This production fuels the growth and reproduction of living marine resources and is a critical factor exerting control over which species produce harvestable surpluses, contributing to fishery yields (Ryther, 1969; Chassot *et al.*, 2010; Stock *et al.*, 2017) and ensuring global food security (Perry, 2011; Christensen *et al.*, 2015). In addition to the production of continental shelf species that are exploited in fisheries, there is also significant trophic transfer between open ocean primary production and mesopelagic fishes on a global basis (Davison *et al.*, 2013; Irigoien *et al.*, 2014). At a more fundamental level, phytoplankton production is the central driver of most marine ecosystems (Sigman & Hain, 2012) and the biogeochemical processes governing carbon flow and export flux (Doney *et al.*, 2014; Laufkotter *et al.*, 2016). However, oceanic photosynthetic production is not constant in time and space; geographic and phenological (bloom timing and duration) variability occurs due to complex biophysical factors controlling phytoplankton blooms owing to the dynamics between the rates of cell reproduction and mortality associated with death and grazing (Behrenfeld & Boss, 2014; Cherkasheva *et al.*, 2014). The variability in blooms affect energy flow from phytoplankton production to pelagic and demersal communities and thus both horizontal and vertical transport of energy in the water column (Corbiere *et al.*, 2007).

Phytoplankton bloom dynamics have been characterized on basin and global scales, identifying differing patterns of bloom phenology by latitude and oceanic province. Analyses of time series change in bloom dynamics complement descriptions of the spatial organization of blooms utilizing a number of different sources of data. For example, a study with a geographic focus in the North Atlantic found that spring bloom timing has advanced for some temperate latitude regions and was delayed in other areas, whereas the fall and winter blooms have been mostly delayed (Taboada & Anadon, 2014). Other longer-term studies identified the effects of changing mixed layer dynamics on the relative strength of spring and fall blooms in the North Atlantic (Martinez *et al.*, 2011) and widespread shifts in bloom phenology associated with broad-scale changes in the coupled atmosphere-ocean system (D'Ortenzio *et al.*, 2012). Some of the most dramatic changes in bloom characteristics and phenology have occurred in the Arctic, where bloom maximums have advanced on the order of fifty days from 1997 to 2009 as a consequence of changes in seasonal ice cover (Kahru *et al.*, 2011). Changes in bloom magnitude and timing alter energy flow in the ecosystem, which in turn impact the growth and reproduction of higher trophic levels in the food web (Cushing, 1990; Hunt *et al.*, 2002; Platt *et al.*, 2003; Schweigert *et al.*, 2013; Malick *et al.*, 2015).

Climate variation can indirectly modify bloom timing and size through mechanisms that influence water column conditions such as the supply and ratio of nutrients and light availability. As climate systems shift in response to anthropogenic forcing, there is a need to understand their impact on bloom dynamics both retrospectively and in a forecasting context. As an example, in the Baltic Sea, investigators found that bloom duration has increased in recent years and associated this change in bloom dynamics to increasing water temperature and declining wind stress, which they attributed to global climate change (Groetsch *et al.*, 2016). Change in climate conditions may act to modify blooms through the direct effects of nutrient supply and grazing; additionally, changing distributions of parasites and viruses associated with climate change will likely play a larger role in the dynamics of blooms and the nature of fixed carbon available to primary grazers (Frenken *et al.*, 2016). Projections of bloom dynamics by global earth system models (e.g., CanESM2, GFDL-ESM2M, HadGEM2-CC, IPSL-CM5A-MR, MPI-ESM-LR, and NEMO-MEDUSA) suggest that regions dominated by seasonal blooms may see diminished bloom events that are replaced by smaller seasonal blooms more typical of contemporary subtropical regions (Henson *et al.*, 2013). Other simulations suggest that future climate will greatly change the nature of seasonal and permanent stratification features, which is one of the more important physical factors controlling the onset and duration of blooms (Holt *et al.*, 2016). Furthermore, direct temperature effects on cell division rates and physiological processes could also influence bloom timing in a warming climate (Hunter-Cevera *et al.*, 2016).

In this manuscript we describe the spatial and temporal dynamics of the dominant phytoplankton blooms of the global ocean. While phytoplankton phenology has been actively investigated, here we define events detected using change-point statistics (Friedland *et al.*, 2015; Friedland *et al.*, 2016) as opposed to other frequently used algorithms which generally rely on threshold methods and curve fitting (Ueyama & Monger, 2005; Ji *et al.*, 2010; Brody *et al.*, 2013; Blondeau-Patissier *et al.*, 2014; Marchese *et al.*, 2017). Furthermore, many of these methods rely on the availability of a full yearly cycle of data, which limits their application at high latitudes due to the missing winter values from satellite data (Cole *et al.*, 2012; Ferreira *et al.*, 2014; Ferreira *et al.*, 2015); noting however, that productive approaches to deal with this issue are emerging (Marchese *et al.*, 2017). The change-point approach provides distinct determinations of bloom start and end, which allows exploration of the internal relationships among bloom characteristics, and represents an area of novelty compared to previous analyses of global, satellite-derived trends in phytoplankton phenology (Kahru *et al.*, 2011; Racault *et al.*, 2012). As will be the case with subsequent analyses, our time series is longer than those used by these previous studies, thus statistics of association and trend are informed by more

data. Using this more mature remote sensing ocean color time series, our analysis examines times series trends in bloom parameters on both regional and global scales, with summary data for specific latitudinal ranges.

METHODS

Chlorophyll data

We analyzed phytoplankton blooms using chlorophyll *a* concentration ([Chl]) data extracted from remote-sensing databases using a global 1° latitudinal/longitudinal grid centered on half degrees. [Chl] was based on measurements made with the Sea-viewing Wide Field of View Sensor (SeaWiFS), Moderate Resolution Imaging Spectroradiometer on the Aqua satellite (MODIS), Medium Resolution Imaging Spectrometer (MERIS), and Visible and Infrared Imaging/Radiometer Suite (VIIRS) sensors. We used the Garver, Siegel, Maritorena Model (GSM) merged data product at 100 km (equivalent to a 1° grid) and 8-day spatial and temporal resolutions, respectively, obtained from the Hermes GlobColour website (hermes.acri.fr/index.php). These four sensors provide an overlapping time series of [Chl] during the period 1998 to 2015 and were combined based on a bio-optical model inversion algorithm (Maritorena *et al.*, 2010). The compiled time series from January 1, 1998 to December 27, 2015, consisted of 828 8-day [Chl] observations for each grid location. There were 38,433 grid locations with sufficient [Chl] to perform at least one bloom determination (at least one run of 23 time steps with 12 [Chl] observations), including some locations that were in inland waters which did not factor into the analysis. Some aspects of the analysis do not include data from high latitudes (>62° N/S) due to the increased frequency of gaps at these latitudes reflecting the limited period of available data during the year and the presence of sea ice and cloud cover, which both obscure ocean color satellite imagery.

Dominant plankton bloom analyses

Seasonal phytoplankton blooms, as evidenced by changes in [Chl], were detected using change-point statistics. In this study, we define a seasonal bloom as a discernable elevation in [Chl], one that is bracketed by distinct start and end points as identified using the change-point algorithm, occurring within a 6-month time frame. For each grid location, the search for bloom events started with the first half-year block of the time series (the first 23 8-day [Chl] measurements), progresses to search for blooms during the next half-year block beginning with the second [Chl] measurement of the year, and

then continues to step through the entire time series. Only half-year series with a minimum of 12 observations were considered for analysis; linear interpolation was used to fill missing values within the range of the data and missing values outside the range were filled with the first and last observations at the beginning or end of the time series, respectively. Hence, for each grid location, 806 bloom determinations were attempted and each detected bloom was associated with one of the 46 search start days of the year (46 bloom detections over the first 17 years of the times series and 24 attempts in the final year). From these data, we identified the search start day of the year that yielded the dominant bloom, which was defined as the search window that yielded the highest number of bloom detections. If more than one start day yielded the highest number of bloom detections, the dates were sorted sequentially and the median day was used as the dominant bloom. With the 38,433 grid locations and factoring 806 bloom determinations per location, ~31 million bloom determinations were attempted.

Blooms were detected using the sequential averaging algorithm called STARS or "sequential *t*-test analysis of regime shifts" (Rodionov, 2004, 2006) which finds the change-points in a time series. STARS algorithm parameters were specified *a priori*: the alpha level used to test for a change in the mean was set to $\alpha = 0.1$; the length criteria, the number of time steps to use when calculating the mean level of a new regime, was set to 5; and, the Huber weight parameter, which determines the relative weighting of outliers in the calculation of the regime mean, was set to 3. A bloom was considered to have occurred if there was a period bracketed by a positive and negative change-point. We ignored change-points (positive or negative) that occurred in the first or last two periods of the time series (8-day periods 1, 2, 22 and 23). The minimum duration of a bloom was three sample periods, which represents the minimum span the algorithm needed to find a positive followed by a negative change-point. This method has been used in previous analyses of US Northeast Shelf (Friedland *et al.*, 2008; Friedland *et al.*, 2015), Arctic (Friedland & Todd, 2012), and North Atlantic bloom patterns (Friedland *et al.*, 2016).

We extracted a suite of statistics to characterize the timing and size of each bloom event. For each location, we calculated bloom frequency as the percentage of years with a detected bloom in study years with sufficient data to do a bloom determination, i.e. some locations may have had persistent cloud cover in a year so a bloom detection could not be attempted. Bloom start was defined as the first day of the year of the bloom period. Bloom duration was defined as the number of days of the bloom period. Bloom intensity was the mean of the [Chl] during the bloom period which carries the unit mg m^{-3} and reflects the biomass of the bloom. Bloom magnitude was the integral of the [Chl] during the bloom period and describes the overall size of the event considering that short and long duration blooms can

have the same intensity. Magnitude can be calculated as the sum of the [Chl] during the blooms, which carries the unit mg m^{-3}; or, as the product of the mean [Chl] during the bloom and the duration in 8-day periods, which carries the unit mg m^{-3} 8-day. We used the latter unit designation to distinguish it from bloom intensity.

Effect of bloom timing on bloom characteristics

For each grid location, we examined the correlation between bloom start and duration, magnitude, and intensity of the dominant bloom. Pearson product-moment correlations were calculated and limited to grid locations with a minimum of eight detected blooms. Significant correlations with a probability level α <0.05 were highlighted in global maps. Given that regressions were performed on a grid cell-by-cell basis, it is possible that multiple testing could have led to excess accumulation of Type I error. However, spatial patterns shown herein generally remain consistent if a different threshold of statistical significance is used.

Trends in bloom parameters

We evaluated the time series changes in bloom parameters using Mann-Kendall non-parametric trend analysis. We calculated Kendall's tau test for the significance (two-tailed test) of a monotonic time series trend (Mann, 1945) for bloom start day, magnitude, intensity and duration of the dominant bloom. We also calculated Theil-Sen slopes of trend, which is the median slope joining all pairs of observations. In addition to absolute Theil-Sen slopes, we also calculated relative Theil-Sen slopes, where the slope is joining each pair of observations divided by the first of the pair before the overall median is taken. Trend tests and slope estimates were limited to grid locations with at least 10 detected blooms. Mean relative Theil-Sen slopes were calculated over 5° latitude and longitude bands excluding data from latitudes north and south of 62°N and 62°S, respectively. Absolute trends, calculated as the product of the absolute Theil-Sen slope and the length of study period, were summarized on a global and regional basis. In addition to the data requirements on number of blooms, outliers, as identified as estimates outside the range of ±2 standard deviations of the mean, were removed. Global mean trends were expressed by trend test probability intervals and cumulative intervals. While individual grid cells with probabilities > 0.05 inevitably have a Theil-Sen slope whose 95% confidence interval overlaps with zero, we nevertheless opted to examine all probability intervals in order to see if any global or regional patterns emerged in the direction and magnitude of the mean Theil-Sen slopes when examined across all grid cells. Probabilities were rounded to intervals of 0.1 such that interval 0.0 includes p<0.05,

interval 0.1 includes 0.05≤p<0.15, etc. The cumulative trends are based on the same data as the interval trends summing data over each progressive probability interval. Regional trends were based on eight subdivisions of the world ocean (see Fig. 1) and the contrast between oligotrophic and non-oligotrophic ocean areas, eutrophic and mesotrophic areas (see: ocean.acri.fr/multicolore for source of oligotrophic ocean mask). These regional trends were presented for probability interval 0.0 and cumulative interval 1.0 only.

Effects of abiotic factors on bloom parameters

We considered a suite of five abiotic factors that may be related to bloom timing and the size of blooms through regionally varying mechanisms. Sea surface temperature (SST) extracted from the NOAA Optimum Interpolation Sea Surface Temperature Analysis datasets (OISST), provides SST with a spatial grid resolution of 1.0° and temporal resolution of 1 month (Reynolds *et al.*, 2002). The dataset uses *in situ* data from ships and buoys as a means of adjusting for biases in satellite data. Salinity, mixed layer depth (MLD), and zonal and meridional wind stress data were extracted from the Ocean Data Assimilation Experiment, which incorporates near-real time data into an ocean model to estimate ocean state parameters (Zhang *et al.*, 2007). The data are distributed on a non-standard global grid (360 longitudinal data points by 200 latitudinal data points) that was resampled to a 1.0° grid resolution and temporal resolution of 1 month. Bloom parameters were correlated to the abiotic factors at monthly (month and year of the bloom) and annual (mean of the year of the bloom) time resolutions for each global grid location. We also calculated relative Theil-Sen slopes of abiotic factors and calculated mean slopes over 5° latitude and longitude bands excluding data from latitudes north and south of 62°N and 62°S, respectively. These latitude and longitude means of the abiotic factors were correlated with the matching latitude and longitude mean relative Theil-Sen slopes of bloom parameters.

RESULTS

Dominant bloom characteristics

The timing and size of the dominant bloom varied globally revealing distinct patterns often associated with latitudinal bands. Bloom frequency had an interquartile range of 67% and 89% over the global ocean (Fig. 2a), which may seem low considering we selected the detection time frame that produced the most bloom detections. An algorithm optimized to find the maximum number of blooms may be expected to detect a bloom in most years. It should be noted that while setting a constraint on bloom

duration was necessary to categorize a spatially and temporally variable phenomenon, this constraint can result in 'missing' blooms. For instance, the bloom duration constraint may underestimate bloom frequency in areas where the dominant bloom tends to be a multi-season event. This can be seen in the North Atlantic frequency data where a segment of the Northeast Atlantic has relatively low bloom frequency; detailed analysis of this region showed the blooms tended to be of long duration often exceeding the duration constraint resulting in non-detection in some years (Friedland *et al.*, 2016). Most of the eastern North Pacific has bloom frequency closer to the lower end of the interquartile range contrasting the distinct latitudinal patterns found in the South Pacific. The South Atlantic and Indian oceans were dominated by high bloom frequencies; however, the highest bloom frequencies at the basin scale appear to be associated with the North Atlantic.

The mean start day of the dominant bloom was arrayed primarily by latitude. At high latitudes in the southern hemisphere, the dominant bloom started near the end of the calendar year typically having start days in the 300s, November-December (Fig. 2b). This coincides with austral spring. Progressing equatorward, start day of blooms at lower latitudes in the southern hemisphere shifted to earlier in the year over an approximate range of day 150 to 250 (June – August), which corresponds to austral winter. North of the equator, there was a band of bloom start days at the end of the calendar year with similar timing to the dominant bloom in the Antarctic. In the temperate Northern Hemisphere, there was a band of spring blooms with start days ranging from approximately day 50-150 (March – May), shifting to summer blooms in the high northern latitudes with start days in the 200s (June – July). Thus, in both hemispheres, there are similar latitudinal patterns where fall/winter blooms are dominant at low-to-mid latitudes and spring/summer blooms occur in subpolar and polar ecosystems.

Bloom magnitude was lowest in the oligotrophic ocean areas and highest in shelf seas and the northern hemisphere. Over much of the north Atlantic and Pacific, bloom magnitude was between 10.0-15.0 mg m^{-3} 8-day [1.0-1.2 log (mg m^{-3} 8-day +1); Fig. 2c]. For the areas of the globe between approximately 40°N to 60°S, bloom magnitude was typically <5.0 mg m^{-3} 8-day [< 0.8 log (mg m^{-3} 8-day+1)], with values in the oligotrophic ocean ranging from 0.5-1.5 mg m^{-3} 8-day [0.2-0.3 log (mg m^{-3} 8-day+1)]. Bloom intensity followed a similar pattern to bloom magnitude with its lowest values in the oligotrophic ocean and highest in shelf seas and the northern hemisphere (see Appendix S1). In the northern hemisphere above 50°N, bloom intensity was approximately 2.0-4.0 mg m^{-3} [0.5-0.7 log (mg m^{-3}+1)] and tended to be between 1.0-1.5 mg m^{-3} [0.3-0.4 log(mg m^{-3}+1)] over the latitude range of 40°N to 60°S. Bloom intensity in the oligotrophic ocean was <0.2 mg m^{-3} [< 0.1 log (mg m^{-3}+1)] in many areas.

Mean bloom duration of the dominant bloom was longest in much of the oligotrophic ocean and shortest in shelf seas and the higher latitude areas of the northern and southern hemispheres. Bloom duration tended to exceed 60 days, or two months, in these oligotrophic ocean areas and was often as short as one month in continental shelf ecosystems (Fig. 2d).

Effect of bloom timing on bloom duration and size

The timing of the dominant bloom was related to multiple measures of bloom size including bloom duration, magnitude, and intensity. Over global scales, bloom timing was negatively correlated to bloom duration, indicating that early blooms lasted longer than blooms that began later in the year (Fig. 3a). Very few grid locations had significant positive correlations (~0.1%) indicative of early blooms of short duration. Instead, fully half (50%) of the global grid was found to have significant negative relationships between bloom start and duration.

The correlation between bloom start and magnitude was less robust (Fig. 3b), but reflected the strong correlation found with duration. Over the global grid, most locations had non-significant correlation between bloom start and magnitude (70%). For those locations with significant correlations, 98% had significant negative correlation indicating that early blooms produced high magnitude blooms. The latter result was most likely related to the underlying correlation between bloom start and duration, as duration is a key component in the calculation of magnitude; longer lasting blooms will likely have higher magnitudes. Locations with significant negative correlations between bloom start and magnitude tended to occur at mid-latitudes in both hemispheres.

The final relationship considered was between bloom timing and intensity. These data produced the weakest correlation field with 82% of the global grid found to be non-significant. Of the significant correlations, 92% were significant positive correlations indicating that later starting blooms were of higher intensity or associated with higher mean [Chl] (Fig. 3c).

Relative trends in bloom parameters

The relative Theil-Sen slopes of the bloom parameters start day, magnitude, intensity, and duration reveal distinct regional and global patterns. Distinct clusters of negative trends in bloom start day (i.e., earlier blooms) can be seen in the southern Pacific, Atlantic, and Indian oceans (Fig. 4a). Distinct clusters of positive trends in bloom magnitude (i.e., increasing magnitude) and bloom intensity (i.e., increases in intensity) can be seen across higher latitudes in both northern and southern hemispheres (Fig. 4b and 4c). Also negative trends in bloom magnitude and intensity were more common at low latitudes. While

present, trends in bloom duration were less spatially coherent making spatial patterns difficult to identify (Fig. 4d).

Averaging relative Thiel-Sen slopes over latitude and longitude bins revealed distinct distributional patterns. Mean relative Thiel-Sen slopes for bloom start day binned over latitude show that slopes tended to be negative over most latitudes with the largest relative change found in the southern hemisphere (Fig. 5a). Mean slopes for magnitude were positive at high latitudes and negative for bands around the equator (Fig. 5c), with positive slopes increasing with latitude. Mean slopes for intensity were arrayed by latitude in a similar fashion to magnitude (Fig. 5e). Mean relative Thiel-Sen slopes for bloom duration tended to be positive over most latitudes with the exception of a group of five high latitude northern bands that were negative indicating a shortening of blooms at these latitudes (Fig. 5g). Mean relative Thiel-Sen slopes for bloom start day binned over longitude show that slopes tended to be negative over most longitudes (Fig. 5b). Mean slopes for magnitude were positive for most longitudes with the exception of a cluster associated with the Indian Ocean (Fig. 5d). Mean slopes for intensity were arrayed by longitude in a similar fashion to magnitude (Fig. 5f). Mean relative Thiel-Sen slopes for bloom duration tended to be positive over most longitudes with the exception of ranges of longitudes associated with Indian and Atlantic oceans (Fig. 5h). Compared to other variables, fewer slopes for bloom duration were significantly different from zero.

Effects of abiotic factors on bloom parameters

Our efforts to detect global scale relationships between abiotic factors and bloom characteristic yielded mixed results. The correlation analysis examining the effect of abiotic factors including SST, salinity, mixed layer depth, and wind stress did not reveal any comprehensive global relationships between these factors and dominant bloom dynamics. The monthly and mean annual correlations are presented in supporting information Appendix S2 (figures s2-1-10). These correlation fields are dominated by grid locations with non-significant correlations. However, some inference on the effect of the abiotic factors may be made by comparing their time series trend patterns to the patterns in time series trends in bloom parameters.

Relative Theil-Sen slopes of trends in SST suggest the most dramatic changes in thermal conditions have occurred at high latitudes associated with changes in patterns of sea ice extent and polar amplification of climate change, noting however that most of these data fall outside the latitude constraints (>62° N/S) used here in most analyses (Fig. 6a). At lower latitudes, SST trends were generally positive with the exception of the parts of the North Atlantic, the western North Pacific, and the eastern

South Pacific. Salinity has changed dramatically in isolated high latitude locations in the North Atlantic, likely related to an increase in Arctic melting, where elsewhere over the global ocean there has been a high degree of variability in salinity (Fig. 6b). Mixed layer depth trends have been mostly positive, and to a higher degree in the southern hemisphere, although a lot of spatial variability in trends is evident in the northern hemisphere (Fig. 6c). Both zonal and meridional wind stress have generally declined globally, with a pattern of zonal wind decline most intense along certain lines of latitude (60° S, 30° S, 0°, 30° N, and 60° N) and meridional decline apparently circumscribing basin-scale oceanic gyres (Figs. 6d&e, respectively). Areas with the most intense declines in zonal wind stress correspond to the transition zones between trade winds and westerly winds.

Trends in abiotic factors were summarized by latitude and longitude in the same manner as bloom parameter trends were summarized in Figure 5. Mean relative Thiel-Sen slopes for SST binned over latitude show that slopes tended to be positive over most latitudes with the largest relative changes found at high latitudes, with a secondary peak just north of the equator (Fig. 7a). SST slopes were also positive over most longitudes with the exception of bands associated with parts of the North Atlantic, the western North Pacific, and the eastern South Pacific (Fig. 7b). SST was positively correlated with bloom intensity and negatively correlated with bloom duration over latitudinal bins whereas it was uncorrelated with bloom start and magnitude (Table 1). There were no significant correlations between SST and bloom parameters arrayed by longitude. There did not appear to be a pattern in the latitudinal distribution of salinity slopes; however, the longitudinal pattern suggests an anomalous freshening of the Indian Ocean compared to other ocean areas (Figs. 7c & d, respectively). Despite weak latitudinal patterns, salinity over latitude was correlated with latitudinal pattern of bloom intensity. The longitudinal patterns of salinity trend were positively correlated with bloom magnitude and duration. Slopes of mixed layer depth are mostly positive over latitudinal intervals, with the higher values at higher latitudes; the only areas with negative slopes were associated with the lower latitudes of the northern hemisphere (Fig. 7e). The increase in mixed layer depth appear highest in the Atlantic Ocean basin compared to other areas based on longitudinal summary of slopes (Fig. 7f). Mixed layer depth trend over latitude was uncorrelated with bloom parameters, but were positively correlated with all four bloom parameter over longitudinal bins. Mean slopes were almost all negative for zonal wind stress, over latitude and longitude, with little evidence of spatial patterns in either data summary (Figs. 7g & h, respectively). The only significant correlation between zonal wind stress and bloom parameter was found with bloom duration over longitude. Likewise, mean meridional wind stresses were almost all negative over latitudes and longitudes; however, there may be some level of patterning in the latitudinal

distribution of mean slopes with the largest change occurring at middle latitudes (Figs. 7i & j, respectively). These changes in meridional wind stress over latitude were negatively correlated with bloom magnitude and intensity. Longitudinal patterns of meridional wind stress trends was negatively correlated with bloom start.

Mean Absolute Trends in bloom parameters

Absolute trends expressed as change in bloom parameters over the study period suggest there have been substantial shifts in bloom timing and size. Bloom start day has shifted on the order of 3 days earlier on a global basis and for regions associated with statistically significant shifts, blooms have advanced on the order of two weeks (Fig. 8a). Bloom magnitude and intensity have both increased on a global basis on the order of 0.3 mg m^{-3} 8-day and 0.05 mg m^{-3}, respectively, which represents about a 10% increase in both parameters (Fig. 8b&c). The increases in these parameters in regions associated with statistically significant shifts have been much greater and on the order of 0.9 mg m^{-3} 8-day and 0.4 mg m^{-3}, respectively, which represents about a 35% increase again for both. Bloom duration has shifted on the order of 2 days longer on a global basis and for regions associated with statistically significant shifts, blooms have lengthened on the order of one week (Fig. 8d).

The bloom absolute trends partitioned by the eight subdivisions of the world ocean and the between oligotrophic and non-oligotrophic ocean areas differed from the global means in a number of ways. Bloom start had negative trends, indicating earlier blooms, in all ocean areas; but, the trend was greater in the southern oceans and in oligotrophic areas (Fig. 9a). For regions associated with statistically significant shifts, the North Atlantic had a positive bloom start trend suggesting that the bloom started approximately five days later, whereas the other ocean areas had negative trends suggesting shifts of 1-3 weeks (Fig. 10a). Bloom magnitude and intensity had positive trends in the northern and southern oceans and between oligotrophic and non-oligotrophic regions (Fig. 9b&c). The tropical ocean areas either had zero or negative trends in these parameters. The pattern of change in magnitude and intensity in the regions associated with statistically significant shifts were nearly identical to the global averages, but the size of the shifts was larger when considering only statistically significant results (Fig. 10b&c). Bloom duration increased in all areas except the North Atlantic and tropical Indian oceans where the trend confidence interval included zero (Fig. 10d). The pattern of change in duration in the regions associated with statistically significant shifts was similar to the global patterns; however, four regions had confidence intervals that included zeros (Fig. 10d).

DISCUSSION

Our analysis of phytoplankton blooms on a global scale suggests directional time series change in the timing, duration, and size of blooms, which portends changes in the functioning of marine ecosystems and carbon cycling from local to basin scales (Ji *et al.*, 2010). Notably, we provide evidence that blooms are initiating earlier in the year, having shifted in timing on the order of weeks in some regions, and are of longer duration suggesting the timing of bloom cessation has also changed. There have also been changes in the pattern of bloom size, suggesting an increase in bloom size at high latitudes and a decrease at low latitudes in a gradated fashion. It is critical to understand these changes in bloom dynamics since they provide labile biomass that form the basis of food webs and are fundamentally important to the biogeochemical functioning of marine ecosystems (Sigman & Hain, 2012).

The low spatial coherence between correlations of the abiotic factors and bloom intensity and magnitude is in stark contrast to the high spatial coherence of global trends in these bloom parameters and time series trends in the abiotic factors, suggesting the importance of variability and local factors in the control of blooms on a global scale. Local changes in salinity and temperature affect stratification, which can trap phytoplankton above the pycnocline and decrease nutrient inputs from deeper layers, while decreased wind-driven mixing will exacerbate this scenario. In a global comparison of the effects of stratification on chlorophyll biomass, Dave and Lozier (2013) showed mixed trends in stratification over much of the globe, with much of the eastern subtropical Pacific experiencing increased stratification, while much of the Atlantic experiencing decreased stratification. However these changes were not well correlated with trends in chlorophyll concentrations, further suggesting the importance of local processes controlling blooms. Similar to the results presented in this study, Dave and Lozier (2013) found trends in decreasing stratification over much of the mid- and lower latitudes, which were driven primarily by increased rates of warming of subsurface water relative to surface waters, resulting in an increased mixed layer depth.

Though clearly not a test of hypotheses, the comparison of latitudinal and longitudinal patterns of trends in potential abiotic forcing factors may offer some insights on both global and regional changes in bloom dynamics. The latitudinal patterns in SST and meridional wind stress trends are similar to the latitudinal pattern in bloom duration in that all show bimodal distributions at low latitudes. This particular pattern is consistent with an increase in bloom duration in the Baltic Sea that also coincided with warming temperatures and decreased winds (Groetsch *et al.*, 2016). Likewise, there are features in the latitudinal pattern of mixed layer depth that match the latitudinal patterns in bloom magnitude and intensity trends. Furthermore, the advance in bloom timing over all latitudes may be related to the

global changes in wind stress. The most striking longitudinal pattern in global bloom dynamics is associated with the Indian Ocean characterized by reductions in bloom magnitude, intensity, and duration corresponding roughly with meridians 50° to 100° E. Phytoplankton dynamics in the Indian Ocean have been considered in the context of abiotic forcing. Goes *et al*. (2005) and Gregg *et al*. (2005) documented increases in net primary production in the western Indian Ocean; however, a more recent study is consistent with our findings, suggesting a reduction in [Chl] over the past 16 years (Roxy *et al.*, 2016). These researchers attributed the change in [Chl] to a reduction in available nutrients in the euphotic zone due to increasing SST that increased stratification-induced trapping of nutrients in the deeper Indian Ocean. The confounding influence of increasing SST trends on mixing and phytoplankton growth rates make prediction of phytoplankton dynamics difficult, especially in the Indian Ocean, an area experiencing the largest warming trend in the tropical ocean (Roxy *et al.*, 2014). However, it is worth noting that the most striking longitudinal pattern in the abiotic data we found was in the salinity data suggesting a freshening of Indian Ocean waters, which may have amplified thermal effects on stratification as described due to changes in monsoon patterns.

A general decrease in zonal and meridional wind stress has the potential to impact production by reducing the wind-driven mixing in areas of light-limited production (Kim *et al.*, 2007). Contrary to this, while our analysis suggests an overall decrease in winds on a broad scale, there is an associated broad increase in the mixed layer depth. This may be due in part to local changes in temperature and salinity affecting stratification. While most regions of the globe are experiencing decreasing wind stress, the few regions where wind stress is increasing are also experiencing the largest increases in mixed layer depth, such as in the southern Atlantic Ocean at 60°S. This is likely a result of higher mean wind speeds in these locations since the power of wind exerted on the water scales with the cube of mean wind speed. Therefore, even a small increase in wind stress in an area can result in profound changes in wind-driven mixing and increased MLD. The global trends in MLD bear a striking resemblance to the global trends in bloom intensity, and to a lesser degree, bloom magnitude. However, the spatial correlations between MLD and these bloom parameters is low and bears few spatially significant regions, save for the oligotrophic southern subtropical Pacific, where enhanced mixing may enhance nutrient concentrations (de Boyer Montegut *et al.*, 2004). In the subpolar and northern subtropical regions of the North Atlantic, Ueyama and Monger (2005) found an inverse relationship between bloom intensity and wind-induced mixing, where decreased mixing during blooms resulted in enhanced bloom intensity, while the opposite was true for the southern subtropical region where nutrients may be limiting production and light penetration is greater. Atmospheric-related variability in wind-driven mixing was

also found to affect the timing of bloom initiation, where the start day of blooms in the North Atlantic was strongly associated with the winter North Atlantic Oscillation index (Ueyama & Monger, 2005). A similar relationship between wind speed and bloom timing has also been detected in the Japan Sea (Yamada & Ishizaka, 2006). Furthermore, Moore *et al.* (2013), in a review of nutrient limitation dynamics in the global ocean, concluded that nitrogen was limiting in much of the surface waters in tropical latitudes, consistent with our observations. In areas where nitrogen is not limiting, iron limitation tends to dominate (e.g., the Southern Ocean and the eastern equatorial Pacific (Behrenfeld *et al.*, 1996)). Iron limitation may play a particularly large role in the differences we observed between the bloom dynamics in the eastern North and South Pacific (Behrenfeld & Kolber, 1999).

Despite methodological differences in bloom detections and analyses, our results do align with those from other global and basin-scale estimates of bloom parameters. Different bloom detection algorithms lead to varying accuracy and precision of bloom phenology metrics (Ferreira *et al.*, 2014); and consequently, varying depictions of bloom dynamics (Brody *et al.*, 2013). Our focus is on the dominant annual bloom occurring within a grid cell and on the main period of elevated bloom conditions constrained by the length of our detection time window. As a number of investigators have characterized (Sapiano *et al.*, 2012; Taboada & Anadon, 2014), most areas of the globe are dominated by a single bloom with the exception of some regions that are characterized by a secondary bloom in regions predominately oriented in specific latitudinal bands. Despite this methodological difference, our characterization of bloom start is similarly patterned to previous global (Racault *et al.*, 2012; Sapiano *et al.*, 2012) and basin scale studies (Henson *et al.*, 2009; Taboada & Anadon, 2014; Zhang *et al.*, 2017). However, our estimates of bloom duration are at variance with most studies owing to the contrast in methods applied between studies. In studies estimating bloom duration using a threshold approach (Siegel *et al.*, 2002), bloom duration tended to be 2-fold longer than ours (Racault *et al.*, 2012; Sapiano *et al.*, 2012). However, the spatial patterns of long versus short bloom duration were consistent with our results. The measures of bloom size, here referred to as magnitude and intensity and variously named and applied by different investigators, were also similar between studies and generally followed climatological patterns of the distribution of [Chl] (Doney *et al.*, 2003).

On a global scale, the spatial organization of areas with homogenous bloom dynamics appears to have a high degree of zonal band patterning and more complex organization associated with meridional bands (Sapiano *et al.*, 2012). For example, mean relative Thiel-Sen slopes for bloom duration tended to be positive over most latitudes with exception of a group of five high latitude northern bands, which were negative indicating a shortening of blooms at these latitudes. Mean slopes for magnitude

and intensity were positive for most longitudes with the exception of a cluster associated with the Indian Ocean.

Changes in bloom timing and size were not uniform over the globe. Owing to contrasts in oceanographically defined functional regions and latitudinal patterns, changes in bloom dynamics will likely have different regional impacts. An analysis of spring and fall blooms in the north Atlantic and Pacific basins that employed a spectral decomposition approach for bloom detection characterized regional scale time series change in bloom timing and magnitude (equivalent to bloom intensity as used here) that hold many similarities to the patterns described in our analysis (Zhang *et al.*, 2017). Bloom timing was alternatively advanced and delayed on the order of weeks with coherent trends in matching areas of both basins. It is difficult to compare our trends in bloom intensity to their results for trends in magnitude since our spatial characterization is based on relative Theil-Sen slopes. Similarly, in a study focused on the North Atlantic, Taboada and Anadon (2014) provided estimates of bloom intensity trends that match our study results; however, their method of estimating bloom timing trends differed from those presented here. Racault *et al.* (2012) estimated trends in bloom duration on a global scale also using linear regression, but with a time series restricted to the length of the SeaWiFS time series only (1998-2007). Their estimates of global trends in bloom duration were mostly negative indicating a tendency for blooms to be shortened over global scales. We note, however, that their time series is shorter than that analyzed here and bloom duration was estimated using a threshold approach (Siegel *et al.*, 2002), which, as noted above, provides estimates of bloom duration 2-fold longer than ours. Hence, they are estimating a different aspect of phytoplankton dynamics, whereas we are focusing on the discrete portion of the bloom associated with highly elevated [Chl].

We view our results in the context of changes that have occurred and will likely occur to the global climate system. Global thermal conditions are changing and it is important to consider change in the level of system variability and its impact on ecosystems (Vazquez *et al.*, 2017). Change in thermal regime is having profound effects on atmospheric circulation and the forcing factors related to bloom development, which may be more important to phytoplankton than the direct effect of change in thermal regime itself (Francis & Vavrus, 2015). The latitudinal changes in bloom magnitude and intensity are also consistent with the effects of global thermal change on phytoplankton community composition (Marinov *et al.*, 2010), shifting communities to include members which are capable of different growth rates or resistance to grazing that allow for a change in [Chl]. Furthermore, changing thermal regimes have been associated with shifting species composition of blooms, where for a fixed study site blooms have become increasingly dominated by the genus *Synechococcus* (Hunter-Cevera *et al.*, 2016). The

changing role of cyanobacteria is expected to have a profound effect on plankton dynamics in a range of aquatic systems (Visser *et al.*, 2016). We can also expect changes to the seasonal nature of blooms (Henson *et al.*, 2013) and likely impacts on secondary production as well (Litchman *et al.*, 2006). The change in dominant bloom timing we observed is consistent with the effect of an increase in global temperature and its role in mixed layer dynamics, though the rate of stratification and turbulent mixing remains unclear (Franks, 2015). These are changes to the base of food web warrant further investigation.

Change in phytoplankton bloom dynamics would be expected to impact the rate of flux of particulate organic carbon (POC) from the water column to the benthos. Parts of the world ocean are dominated by production cycles that are characterized by blooms associated with high concentrations of biomass whereas other regions have bloom features that are not as prominent, though in many cases primary production can still be at a high level (Reygondeau *et al.*, 2013). However, phytoplankton blooms, in particular, support conditions that result in the intense flux of POC (Reigstad *et al.*, 2011; Belley *et al.*, 2016). It follows that changes in the timing and size of a bloom will affect the amount of POC exported to the benthos. Over most regions of the globe, blooms appear to have lasted longer, which could result in an increase in POC flux. Bloom magnitude and intensity have changed over latitudinal ranges, most notably with decreased bloom magnitude at low latitude and increases at high latitudes. Similar changes in bloom magnitude across a range of latitudes were obtained in a study that used an earth system model that included data assimilation to examine changes in North Pacific bloom characteristics since the 1960s (Asch, 2013). Together these results indicate that POC fluxes to the benthos may increase at high latitudes, while decreasing at lower latitudes. These changes in bloom dynamics should be taken into account in global carbon flux estimation models.

Species composition of phytoplankton communities varies over global scales and is principally influenced by dispersion and competitive exclusion (Barton *et al.*, 2010). However, species composition is also influenced by environmental conditions, such as mixing regimes and light conditions, (Barton *et al.*, 2015) leading to concerns that shifting thermal conditions will actuate shifts to smaller size taxa (Moran *et al.*, 2010). These smaller producers have different dynamics and vertical transport properties, which have the potential to affect both export flux and the way an ecosystem functions (Mouw *et al.*, 2016). Utilizing phytoplankton size estimated from remote sensing data (Kostadinov *et al.*, 2016; Mouw *et al.*, 2017), Mouw *et al*. (2016) contrasted the difference in export flux and transfer efficiency during times dominated by small and large cells within biogeochemical provinces. They found periods dominated by small cells to have both greater export flux efficiency and lower transfer efficiency than

periods dominated by large cells. Rising temperatures will likely shift phytoplankton niches poleward and are predicted to have the greatest potential impact on tropical phytoplankton diversity (Thomas *et al.*, 2012). Considering the importance of species groups to the role of phytoplankton production, the phenology of various methods to determine phytoplankton size has been compared (Kostadinov *et al.*, 2017) and the phenology of some methods has been connected to environmental conditions (Cabré *et al.*, 2016; Soppa *et al.*, 2016). However, the changes in phenology of various phytoplankton groups have yet to be explored, which could provide refinements to both retrospective and forecasted modelling efforts.

This study provides substantial evidence to support the observation that early blooms are longer lasting blooms and conversely delayed bloom start is associated with shorter blooms. This phenomenon has been described previously on a global scale (Racault *et al.*, 2012) and for the North Atlantic (Friedland *et al.*, 2016), with the latter study exploring the hypothesis that bloom duration is in large measure shaped by grazing by zooplankton that have a diapause life cycle. It is important to note that despite using a different bloom measurement methodology, results from Racault *et al*. (2012) and for the North Atlantic (Friedland *et al.*, 2016) agree with the current study in the overall nature of the relationship (i.e., the direction of trends and coherence at large spatial scales), but differ in the fine scale regional patterning of this correlation. It may be through this regional patterning that we are able to evaluate the relative role of nutrient limitation and grazing in shaping bloom development (Evans & Parslow, 1985; Fasham *et al.*, 1990). The latitudinal banding of this relationship would have to be reflected in the nature of pre-bloom mixing and initial nutrient supply over a range of physical environments for nutrient supply to be the unifying factor controlling bloom duration as a function of bloom initiation. This work has yet to be done, but in a practical sense has a better chance of being accomplished considering the paucity of grazing information in most parts of the world ocean.

The observational results of this study provide some level of validation for earth systems models that simulate global climate and ocean systems dynamics. Multiple earth system models suggest that climate change will have the greatest impact on bloom phenology at high latitudes (Henson *et al.*, 2013). Under a business-as-usual emissions scenario, the month of maximum primary productivity is projected to advance by 0.5-1 months by the end of the 21st century across many ocean ecosystems. The exception to this pattern is the oligotrophic subtropical gyres where delays in the timing of peak primary production have been projected. These changes have been attributed to earlier easing of light limitation due to increases in stratification (Henson *et al.*, 2013). These future projections utilize earth system model outputs with a monthly resolution, so additional research that can detect finer scale changes in

phenology is needed. One study that used finer temporal resolution data from the NCAR Community Earth System Model (CESM) model assimilated historical data on atmospheric observations and sea surface temperature (Asch, 2013). In contrast to models of future projections, this study of historical patterns identified the largest trends in bloom phenology in oligotrophic areas (Asch, 2013), which may reflect an influence of inter-annual climate variability rather than climate change. Our observational results are consistent with this pattern, and thus provide an indication of the skill of the NCAR model, which did not assimilate any ocean color data.

As ocean color time series have grown in length, there have been efforts to describe time series trends in bloom characteristics. Importantly, these efforts have included disciplined analyses of the requirements to detect trends in the face of noisy and incomplete data and whether trends can be attributed to climate change or not (Beaulieu *et al.*, 2013; Henson *et al.*, 2016). Furthermore, Henson *et al.* (2013) estimates that it would require ~ 30 years of data to distinguish trends in bloom phenology from natural decadal variability. Given the results of these investigations, we approach our findings with caution. As encouraging as it is to now have a nearly twenty-year time series of data, it is difficult to be conclusive about the description of trends and to attribute any of these trends to climate change. However, it is reasonable to compare these trends to observed climate variation over the past two decades and discuss whether these trends are consistent with future projections under different climate change scenarios.

CONCLUSIONS

The timing and size of phytoplankton blooms have changed on both regional and global scales. This finding is important because blooms play a pivotal role in the flow of energy in marine ecosystems, impacting the way food webs work and the way these ecosystems provide a range of services. The dominant bloom was found to vary with latitude and in localized patterns associated with specific oceanographic features. Blooms have increased in magnitude and intensity at high latitudes and decreased in equatorial areas. Overall, blooms started earlier and lasted longer, with bloom timing having the most profound effect on bloom duration; early blooms tended to last longer than later starting blooms. This finding has the potential to impact phenological relationships between producer and consumer species such as mesozooplankton and higher trophic position fish and invertebrates. Timing mechanisms for reproduction in many species have evolved that ensure adequate forage for early life stages, which may be impacted by changes in bloom timing. In regions where blooms last longer and are associated with higher [Chl], the dynamics of the biological pump are likely to alter the

rates of carbon cycling and export. A shift to earlier bloom timing is consistent with the expected effect of warming ocean conditions seen in recent decades. It is incumbent upon assessment and modelling practitioners to account for the dynamic variability of phytoplankton production.

ACKNOWLEDGEMENTS

We thank C. Stock and M. Scharfe for comments on an early draft of the paper and GlobColour (http://globcolour.info) for the data used in this study that has been developed, validated, and distributed by ACRI-ST, France.

Data Accessibility Statement

All chlorophyll concentration data is available as NCDF files from the GlobColour products databased located at: http://hermes.acri.fr/?class=archive. Ocean Data Assimilation Experiment data is located at: https://www.gfdl.noaa.gov/ocean-data-assimilation.

Biosketch

Kevin Friedland is a researcher with the National Marine Fisheries Service at the Narragansett Laboratory in Rhode Island, USA. He holds a bachelors degree in ecology from Rutgers College in New Jersey and a doctorate from the College of William and Mary in Virginia. His dissertation research was on the distribution and feeding ecology of Atlantic menhaden. During his professional career, he has done research on menhaden, bluefish, sea herring, sturgeon, eel, cod, haddock, and salmon. His publications cover a range of topics including: estuarine ecology of fishes, functional morphology, feeding ecology, recruitment processes, fisheries oceanography, stock identification, ecosystem ecology, and climate change. His current research is on the effects of bloom phenology on ecosystem function. He has served as the chair of several International Council for the Exploration of the Sea (ICES) scientific working groups and is currently the US representative to SCICOM.

REFERENCES

Asch, R.G. (2013) Interannual-to-Decadal Changes in Phytoplankton Phenology, Fish Spawning Habitat, and Larval Fish Phenology. *Ph.D. dissertation, University of California, San Diego. 268 p.*,

Barton, A.D., Lozier, M.S. & Williams, R.G. (2015) Physical controls of variability in North Atlantic phytoplankton communities. *Limnology and Oceanography*, **60**, 181-197.
Barton, A.D., Dutkiewicz, S., Flierl, G., Bragg, J. & Follows, M.J. (2010) Patterns of diversity in marine phytoplankton. *Science*, **327**, 1509-1511.
Beaulieu, C., Henson, S.A., Sarmiento, J.L., Dunne, J.P., Doney, S.C., Rykaczewski, R.R. & Bopp, L. (2013) Factors challenging our ability to detect long-term trends in ocean chlorophyll. *Biogeosciences*, **10**, 2711-2724.
Behrenfeld, M.J. & Kolber, Z.S. (1999) Widespread iron limitation of phytoplankton in the South Pacific Ocean. *Science*, **283**, 840-843.
Behrenfeld, M.J. & Boss, E.S. (2014) Resurrecting the ecological underpinnings of ocean plankton blooms. *Annual Review of Marine Science, Vol 6, 2014*, **6**, 167-U208.
Behrenfeld, M.J., Bale, A.J., Kolber, Z.S., Aiken, J. & Falkowski, P.G. (1996) Confirmation of iron limitation of phytoplankton photosynthesis in the equatorial Pacific Ocean. *Nature*, **383**, 508-511.
Belley, R., Snelgrove, P.V.R., Archambault, P. & Juniper, S.K. (2016) Environmental drivers of benthic flux variation and ecosystem functioning in Salish Sea and Northeast Pacific sediments. *Plos One*, **11**
Blondeau-Patissier, D., Gower, J.F.R., Dekker, A.G., Phinn, S.R. & Brando, V.E. (2014) A review of ocean color remote sensing methods and statistical techniques for the detection, mapping and analysis of phytoplankton blooms in coastal and open oceans. *Progress in Oceanography*, **123**, 123-144.
Brody, S.R., Lozier, M.S. & Dunne, J.P. (2013) A comparison of methods to determine phytoplankton bloom initiation. *Journal of Geophysical Research-Oceans*, **118**, 2345-2357.
Cabré, A., Shields, D., Marinov, I. & Kostadinov, T.S. (2016) Phenology of size-partitioned phytoplankton carbon-biomass from ocean color remote sensing and CMIP5 models. *Front. Mar. Sci.*, **3**, 591–20.
Chassot, E., Bonhommeau, S., Dulvy, N.K., Melin, F., Watson, R., Gascuel, D. & Le Pape, O. (2010) Global marine primary production constrains fisheries catches. *Ecology Letters*, **13**, 495-505.
Cherkasheva, A., Bracher, A., Melsheimer, C., Koberle, C., Gerdes, R., Nothig, E.M., Bauerfeind, E. & Boetius, A. (2014) Influence of the physical environment on polar phytoplankton blooms: A case study in the Fram Strait. *Journal of Marine Systems*, **132**, 196-207.
Christensen, V., Coll, M., Buszowski, J., Cheung, W.W.L., Frolicher, T., Steenbeek, J., Stock, C.A., Watson, R.A. & Walters, C.J. (2015) The global ocean is an ecosystem: simulating marine life and fisheries. *Global Ecology and Biogeography*, **24**, 507-517.
Cole, H., Henson, S., Martin, A. & Yool, A. (2012) Mind the gap: The impact of missing data on the calculation of phytoplankton phenology metrics. *Journal of Geophysical Research-Oceans*, **117**
Corbiere, A., Metzl, N., Reverdin, G., Brunet, C. & Takahashi, A. (2007) Interannual and decadal variability of the oceanic carbon sink in the North Atlantic subpolar gyre. *Tellus Series B-Chemical and Physical Meteorology*, **59**, 168-178.
Cushing, D.H. (1990) Plankton production and year-class strength in fish populations - an update of the match mismatch hypothesis. *Advances in Marine Biology*, **26**, 249-293.
D'Ortenzio, F., Antoine, D., Martinez, E. & d'Alcala, M.R. (2012) Phenological changes of oceanic phytoplankton in the 1980s and 2000s as revealed by remotely sensed ocean-color observations. *Global Biogeochemical Cycles*, **26**
Dave, A.C. & Lozier, M.S. (2013) Examining the global record of interannual variability in stratification and marine productivity in the low-latitude and mid-latitude ocean. *Journal of Geophysical Research-Oceans*, **118**, 3114-3127.
Davison, P.C., Checkley, D.M., Koslow, J.A. & Barlow, J. (2013) Carbon export mediated by mesopelagic fishes in the northeast Pacific Ocean. *Progress in Oceanography*, **116**, 14-30.

de Boyer Montegut, C., Madec, G., Fischer, A.S., Lazar, A. & Iudicone, D. (2004) Mixed layer depth over the global ocean: An examination of profile data and a profile-based climatology. *Journal of Geophysical Research-Oceans*, **109**

Doney, S.C., Bopp, L. & Long, M.C. (2014) Historical and future trends in ocean climate and biogeochemistry. *Oceanography*, **27**, 108-119.

Doney, S.C., Glover, D.M., McCue, S.J. & Fuentes, M. (2003) Mesoscale variability of Sea-viewing Wide Field-of-view Sensor(SeaWiFS) satellite ocean color: Global patterns and spatial scales. *Journal of Geophysical Research-Oceans*, **108**

Evans, G.T. & Parslow, J.S. (1985) A model of annual plankton cycles. *Biol. Oceanogr.*, **3**, 327–347.

Fasham, M.J.R., Ducklow, H.W. & Mckelvie, S.M. (1990) A nitrogen-based model of plankton dynamics in the oceanic mixed layer. *Journal of Marine Research*, **48**, 591-639.

Ferreira, A.S., Visser, A.W., MacKenzie, B.R. & Payne, M.R. (2014) Accuracy and precision in the calculation of phenology metrics. *Journal of Geophysical Research-Oceans*, **119**, 8438-8453.

Ferreira, A.S.A., Hatun, H., Counillon, F., Payne, M.R. & Visser, A.W. (2015) Synoptic-scale analysis of mechanisms driving surface chlorophyll dynamics in the North Atlantic. *Biogeosciences*, **12**, 3641-3653.

Field, C.B., Behrenfeld, M.J., Randerson, J.T. & Falkowski, P. (1998) Primary production of the biosphere: Integrating terrestrial and oceanic components. *Science*, **281**, 237-240.

Francis, J.A. & Vavrus, S.J. (2015) Evidence for a wavier jet stream in response to rapid Arctic warming. *Environmental Research Letters*, **10**

Franks, P.J.S. (2015) Has Sverdrup's critical depth hypothesis been tested? Mixed layers vs. turbulent layers. *Ices Journal of Marine Science*, **72**, 1897-1907.

Frenken, T., Velthuis, M., Domis, L.N.D., Stephan, S., Aben, R., Kosten, S., van Donk, E. & Van de Waal, D.B. (2016) Warming accelerates termination of a phytoplankton spring bloom by fungal parasites. *Global Change Biology*, **22**, 299-309.

Friedland, K.D. & Todd, C.D. (2012) Changes in Northwest Atlantic Arctic and Subarctic conditions and the growth response of Atlantic salmon. *Polar Biology*, **35**, 593-609.

Friedland, K.D., Hare, J.A., Wood, G.B., Col, L.A., Buckley, L.J., Mountain, D.G., Kane, J., Brodziak, J., Lough, R.G. & Pilskaln, C.H. (2008) Does the fall phytoplankton bloom control recruitment of Georges Bank haddock, *Melanogrammus aeglefinus*, through parental condition? *Canadian Journal of Fisheries and Aquatic Sciences*, **65**, 1076-1086.

Friedland, K.D., Leaf, R.T., Kane, J., Tommasi, D., Asch, R.G., Rebuck, N., Ji, R., Large, S.I., Stock, C. & Saba, V.S. (2015) Spring bloom dynamics and zooplankton biomass response on the US Northeast Continental Shelf. *Continental Shelf Research*, **102**, 47-61.

Friedland, K.D., Record, N.R., Asch, R.G., Kristiansen, T., Saba, V.S., Drinkwater, K.F., Henson, S., Leaf, R.T., Morse, R.E., Johns, D.G., Large, S.I., Hjøllo, S.S., Nye, J.A., Alexander, M.A. & Ji, R. (2016) Seasonal phytoplankton blooms in the North Atlantic linked to the overwintering strategies of copepods. *Elementa*, **DOI: http://doi.org/10.12952/journal.elementa.000099**, p.99.

Goes, J.I., Thoppil, P.G., Gomes, H.D. & Fasullo, J.T. (2005) Warming of the Eurasian landmass is making the Arabian Sea more productive. *Science*, **308**, 545-547.

Gregg, W.W., Casey, N.W. & McClain, C.R. (2005) Recent trends in global ocean chlorophyll. *Geophysical Research Letters*, **32**

Groetsch, P.M.M., Simis, S.G.H., Eleveld, M.A. & Peters, S.W.M. (2016) Spring blooms in the Baltic Sea have weakened but lengthened from 2000 to 2014. *Biogeosciences*, **13**, 4959-4973.

Henson, S., Cole, H., Beaulieu, C. & Yool, A. (2013) The impact of global warming on seasonality of ocean primary production. *Biogeosciences*, **10**, 4357-4369.

Henson, S.A., Dunne, J.P. & Sarmiento, J.L. (2009) Decadal variability in North Atlantic phytoplankton blooms. *Journal of Geophysical Research-Oceans*, **114 Doi 10.1029/2008jc005139**

Henson, S.A., Beaulieu, C. & Lampitt, R. (2016) Observing climate change trends in ocean biogeochemistry: when and where. *Global Change Biology*, **22**, 1561-1571.

Holt, J., Schrum, C., Cannaby, H., Daewel, U., Allen, I., Artioli, Y., Bopp, L., Butenschon, M., Fach, B.A., Harle, J., Pushpadas, D., Salihoglu, B. & Wakelin, S. (2016) Potential impacts of climate change on the primary production of regional seas: A comparative analysis of five European seas. *Progress in Oceanography*, **140**, 91-115.

Hunt, G.L., Stabeno, P., Walters, G., Sinclair, E., Brodeur, R.D., Napp, J.M. & Bond, N.A. (2002) Climate change and control of the southeastern Bering Sea pelagic ecosystem. *Deep-Sea Research Part Ii-Topical Studies in Oceanography*, **49**, 5821-5853.

Hunter-Cevera, K.R., Neubert, M.G., Olson, R.J., Solow, A.R., Shalapyonok, A. & Sosik, H.M. (2016) Physiological and ecological drivers of early spring blooms of a coastal phytoplankter. *Science*, **354**, 326-329.

Irigoien, X., Klevjer, T.A., Rostad, A., Martinez, U., Boyra, G., Acuna, J.L., Bode, A., Echevarria, F., Gonzalez-Gordillo, J.I., Hernandez-Leon, S., Agusti, S., Aksnes, D.L., Duarte, C.M. & Kaartvedt, S. (2014) Large mesopelagic fishes biomass and trophic efficiency in the open ocean. *Nature Communications*, **5**

Ji, R.B., Edwards, M., Mackas, D.L., Runge, J.A. & Thomas, A.C. (2010) Marine plankton phenology and life history in a changing climate: current research and future directions. *Journal of Plankton Research*, **32**, 1355-1368.

Kahru, M., Brotas, V., Manzano-Sarabia, M. & Mitchell, B.G. (2011) Are phytoplankton blooms occurring earlier in the Arctic? *Global Change Biology*, **17**, 1733-1739.

Kim, H.C., Yoo, S.J. & Oh, I.S. (2007) Relationship between phytoplankton bloom and wind stress in the sub-polar frontal area of the Japan/East Sea. *Journal of Marine Systems*, **67**, 205-216.

Kostadinov, T.S., Milutinovic, S., Marinov, I. & Cabre, A. (2016) Carbon-based phytoplankton size classes retrieved via ocean color estimates of the particle size distribution. *Ocean Science*, **12**, 561-575.

Kostadinov, T.S., Cabré, A., Vedantham, H., Marinov, I., Bracher, A., Brewin, R.J.W., Bricaud, A., Hirata, T., Hirawake, T., Hardman-Mountford, N.J., Mouw, C., Roy, S. & Uitz, J. (2017) Inter-comparison of phytoplankton functional type phenology metrics derived from ocean color algorithms and Earth System Models. *Remote Sensing of Environment*, **190**, 162-177.

Laufkotter, C., Vogt, M., Gruber, N., Aumont, O., Bopp, L., Doney, S.C., Dunne, J.P., Hauck, J., John, J.G., Lima, I.D., Seferian, R. & Volker, C. (2016) Projected decreases in future marine export production: the role of the carbon flux through the upper ocean ecosystem. *Biogeosciences*, **13**, 4023-4047.

Litchman, E., Klausmeier, C.A., Miller, J.R., Schofield, O.M. & Falkowski, P.G. (2006) Multi-nutrient, multi-group model of present and future oceanic phytoplankton communities. *Biogeosciences*, **3**, 585-606.

Malick, M.J., Cox, S.P., Mueter, F.J. & Peterman, R.M. (2015) Linking phytoplankton phenology to salmon productivity along a north-south gradient in the Northeast Pacific Ocean. *Canadian Journal of Fisheries and Aquatic Sciences*, **72**, 697-708.

Mann, H.B. (1945) Nonparametric tests against trend. *Econometrica* **13**

Marchese, C., Albouy, C., Tremblay, J.-É., Dumont, D., D'Ortenzio, F., Vissault, S. & Bélanger, S. (2017) Changes in phytoplankton bloom phenology over the North Water (NOW) polynya: a response to changing environmental conditions. *Polar Biology*,

Marinov, I., Doney, S.C. & Lima, I.D. (2010) Response of ocean phytoplankton community structure to climate change over the 21st century: partitioning the effects of nutrients, temperature and light. *Biogeosciences*, **7**, 3941-3959.

Maritorena, S., d'Andon, O.H.F., Mangin, A. & Siegel, D.A. (2010) Merged satellite ocean color data products using a bio-optical model: Characteristics, benefits and issues. *Remote Sensing of Environment*, **114**, 1791-1804.

Martinez, E., Antoine, D., D'Ortenzio, F. & Montegut, C.D. (2011) Phytoplankton spring and fall blooms in the North Atlantic in the 1980s and 2000s. *Journal of Geophysical Research-Oceans*, **116**

Moore, C.M., Mills, M.M., Arrigo, K.R., Berman-Frank, I., Bopp, L., Boyd, P.W., Galbraith, E.D., Geider, R.J., Guieu, C., Jaccard, S.L., Jickells, T.D., La Roche, J., Lenton, T.M., Mahowald, N.M., Maranon, E., Marinov, I., Moore, J.K., Nakatsuka, T., Oschlies, A., Saito, M.A., Thingstad, T.F., Tsuda, A. & Ulloa, O. (2013) Processes and patterns of oceanic nutrient limitation. *Nature Geoscience*, **6**, 701-710.

Moran, X.A.G., Lopez-Urrutia, A., Calvo-Diaz, A. & Li, W.K.W. (2010) Increasing importance of small phytoplankton in a warmer ocean. *Global Change Biology*, **16**, 1137-1144.

Mouw, C., Hardman-Mountford, N., Alvain, S., Bracher, A., Brewin, R., Bricaud, A., Ciotti, A., Devred, E., Fujiwara, A., Hirata, T., Hirawake, T., Kostadinov, T., Roy, S. & Uitz, J. (2017) A Consumer's Guide to Satellite Remote Sensing of Multiple Phytoplankton Groups in the Global Ocean. *Frontiers in Marine Science*, **4**

Mouw, C.B., Barnett, A., McKinley, G.A., Gloege, L. & Pilcher, D. (2016) Phytoplankton size impact on export flux in the global ocean. *Global Biogeochemical Cycles*, **30**, 1542-1562.

Perry, R.I. (2011) Potential impacts of climate change on marine wild capture fisheries: an update. *Journal of Agricultural Science*, **149**, 63-75.

Platt, T., Fuentes-Yaco, C. & Frank, K.T. (2003) Spring algal bloom and larval fish survival. *Nature*, **423**, 398-399.

Racault, M.F., Le Quere, C., Buitenhuis, E., Sathyendranath, S. & Platt, T. (2012) Phytoplankton phenology in the global ocean. *Ecological Indicators*, **14**, 152-163.

Reigstad, M., Carroll, J., Slagstad, D., Ellingsen, I. & Wassmann, P. (2011) Intra-regional comparison of productivity, carbon flux and ecosystem composition within the northern Barents Sea. *Progress in Oceanography*, **90**, 33-46.

Reygondeau, G., Longhurst, A., Martinez, E., Beaugrand, G., Antoine, D. & Maury, O. (2013) Dynamic biogeochemical provinces in the global ocean. *Global Biogeochemical Cycles*, **27**, 1046-1058.

Reynolds, R.W., Rayner, N.A., Smith, T.M., Stokes, D.C. & Wang, W.Q. (2002) An improved in situ and satellite SST analysis for climate. *Journal of Climate*, **15**, 1609-1625.

Rodionov, S.N. (2004) A sequential algorithm for testing climate regime shifts. *Geophysical Research Letters*, **31**, Doi 10.1029/2004gl019448.

Rodionov, S.N. (2006) Use of prewhitening in climate regime shift detection. *Geophysical Research Letters*, **33**, Doi 10.1029/2006gl025904.

Roxy, M.K., Ritika, K., Terray, P. & Masson, S. (2014) The Curious Case of Indian Ocean Warming. *Journal of Climate*, **27**, 8501-8509.

Roxy, M.K., Modi, A., Murtugudde, R., Valsala, V., Panickal, S., Kumar, S.P., Ravichandran, M., Vichi, M. & Levy, M. (2016) A reduction in marine primary productivity driven by rapid warming over the tropical Indian Ocean. *Geophysical Research Letters*, **43**, 826-833.

Ryther, J.H. (1969) Photosynthesis and fish production in the sea. *Science*, **166**, 72–76.

Sapiano, M.R.P., Brown, C.W., Uz, S.S. & Vargas, M. (2012) Establishing a global climatology of marine phytoplankton phenological characteristics. *Journal of Geophysical Research-Oceans*, **117**

Schweigert, J.F., Thompson, M., Fort, C., Hay, D.E., Therriault, T.W. & Brown, L.N. (2013) Factors linking Pacific herring (*Clupea pallasi*) productivity and the spring plankton bloom in the Strait of Georgia, British Columbia, Canada. *Progress in Oceanography*, **115**, 103-110.

Siegel, D.A., Doney, S.C. & Yoder, J.A. (2002) The North Atlantic spring phytoplankton bloom and Sverdrup's critical depth hypothesis. *Science*, **296**, 730-733.

Sigman, D.M. & Hain, M.P. (2012) The Biological Productivity of the Ocean. *Nature Education*, **3**, 1-16.
Soppa, M.A., Volker, C. & Bracher, A. (2016) Diatom phenology in the Southern Ocean: mean patterns, trends and the role of climate oscillations. *Remote Sensing*, **8**
Stock, C.A., John, J.G., Rykaczewski, R.R., Asch, R.G., Cheung, W.W.L., Dunne, J.P., Friedland, K.D., Lam, V.W.Y., Sarmiento, J.L. & Watson, R.A. (2017) Reconciling fisheries catch and ocean productivity. *Proceedings of the National Academy of Sciences of the United States of America*, **114**, E1441-E1449.
Taboada, F.G. & Anadon, R. (2014) Seasonality of North Atlantic phytoplankton from space: impact of environmental forcing on a changing phenology (1998-2012). *Global Change Biology*, **20**, 698-712.
Thomas, M.K., Kremer, C.T., Klausmeier, C.A. & Litchman, E. (2012) A global pattern of thermal adaptation in marine phytoplankton. *Science*, **338**, 1085-1088.
Ueyama, R. & Monger, B.C. (2005) Wind-induced modulation of seasonal phytoplankton blooms in the North Atlantic derived from satellite observations. *Limnology and Oceanography*, **50**, 1820-1829.
Vazquez, D.P., Gianoli, E., Morris, W.F. & Bozinovic, F. (2017) Ecological and evolutionary impacts of changing climatic variability. *Biological Reviews*, **92**, 22-42.
Visser, P.M., Verspagen, J.M.H., Sandrini, G., Stal, L.J., Matthijs, H.C.P., Davis, T.W., Paerl, H.W. & Huisman, J. (2016) How rising CO2 and global warming may stimulate harmful cyanobacterial blooms. *Harmful Algae*, **54**, 145-159.
Yamada, K. & Ishizaka, J. (2006) Estimation of interdecadal change of spring bloom timing, in the case of the Japan Sea. *Geophysical Research Letters*, **33**
Zhang, M., Zhang, Y.L., Qiao, F.L., Deng, J. & Wang, G. (2017) Shifting trends in bimodal phytoplankton blooms in the North Pacific and North Atlantic oceans from space with the Holo-Hilbert spectral analysis. *Ieee Journal of Selected Topics in Applied Earth Observations and Remote Sensing*, **10**, 57-64.
Zhang, S., Harrison, M.J., Rosati, A. & Wittenberg, A. (2007) System design and evaluation of coupled ensemble data assimilation for global oceanic climate studies. *Monthly Weather Review*, **135**, 3541-3564.

Table 1 Pearson product-moment correlation between mean relative Theil-Sen slope binned by 5° latitude and longitude groupings of bloom parameters start day, magnitude, intensity, and duration and abiotic factors sea surface temperature, salinity, mixed layer depth, zonal wind stress, and meridional wind stress. Significant correlations shown in bold.

		SST		Salinity		MLD		u-wind		v-wind	
		r	p	r	p	r	p	r	p	r	p
Latitude	Start	0.173	0.429	0.159	0.447	-0.103	0.626	0.034	0.872	0.014	0.946
	Magnitude	0.345	0.107	0.336	0.100	0.201	0.334	-0.230	0.269	***-0.576***	***0.003***
	Intensity	***0.576***	***0.004***	***0.428***	***0.033***	0.386	0.056	-0.265	0.200	***-0.571***	***0.003***
	Duration	***-0.656***	***0.001***	-0.128	0.543	-0.241	0.246	0.075	0.722	0.091	0.665
Longitude	Start	-0.074	0.534	0.185	0.117	***0.303***	***0.009***	-0.116	0.327	***-0.364***	***0.002***
	Magnitude	0.066	0.579	***0.334***	***0.004***	***0.338***	***0.003***	0.124	0.298	0.053	0.654
	Intensity	0.026	0.826	0.210	0.074	***0.286***	***0.014***	0.006	0.960	0.224	0.057
	Duration	0.072	0.547	***0.382***	***0.001***	***0.239***	***0.042***	***0.343***	***0.003***	-0.193	0.101

Figure 1 Global map showing the extent of 1° latitudinal/longitudinal grid locations with at least 10 years with detected blooms color coded by eight subdivisions of the world ocean. Latitude limits of tropical subdivisions approximate the Tropic of Cancer and Capricorn. Red stippling marks grid locations representing oligotrophic ocean areas.

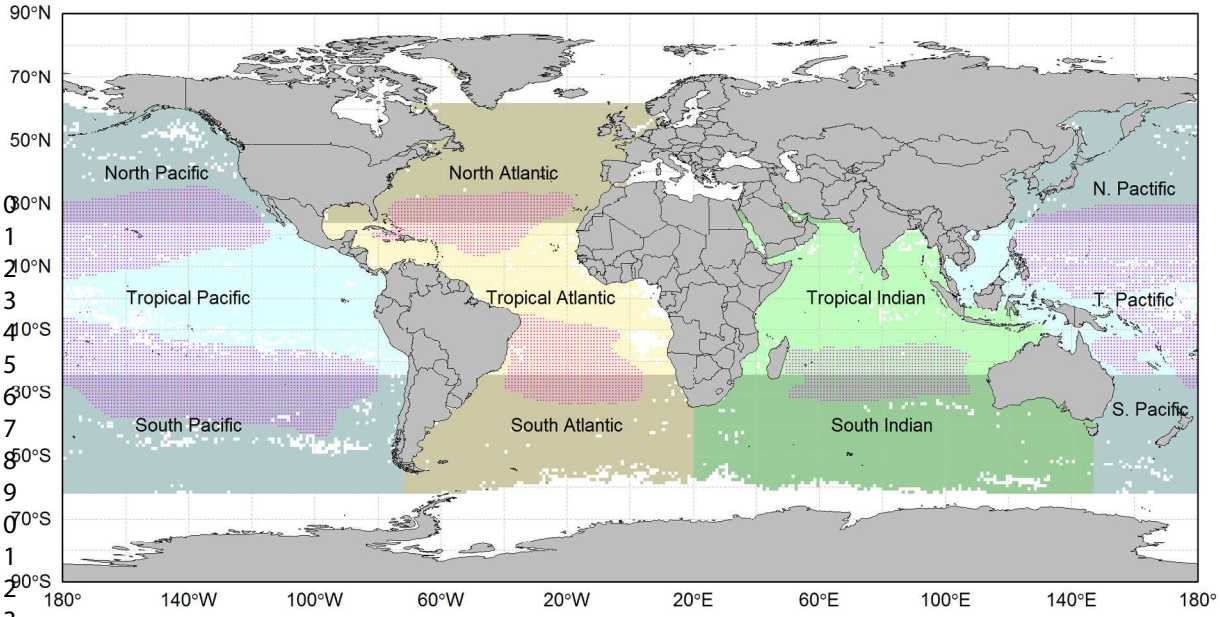

Figure 2 Bloom frequency (a), start day (b), magnitude (c), and duration (d) for the dominant annual bloom based on a global 1° latitudinal/longitudinal grid over the study period 1998-2015. Units: bloom frequency (percentage); bloom start day (day of the year), Day/Date: 50/Feb 19, 100/Apr 9, 150/May 29, 200/Jul 18, 250/Sep 6, 300/Oct 26, 350/Dec 15; bloom magnitude [log (mg m^{-3} 8-day+1)]; and, bloom duration (days).

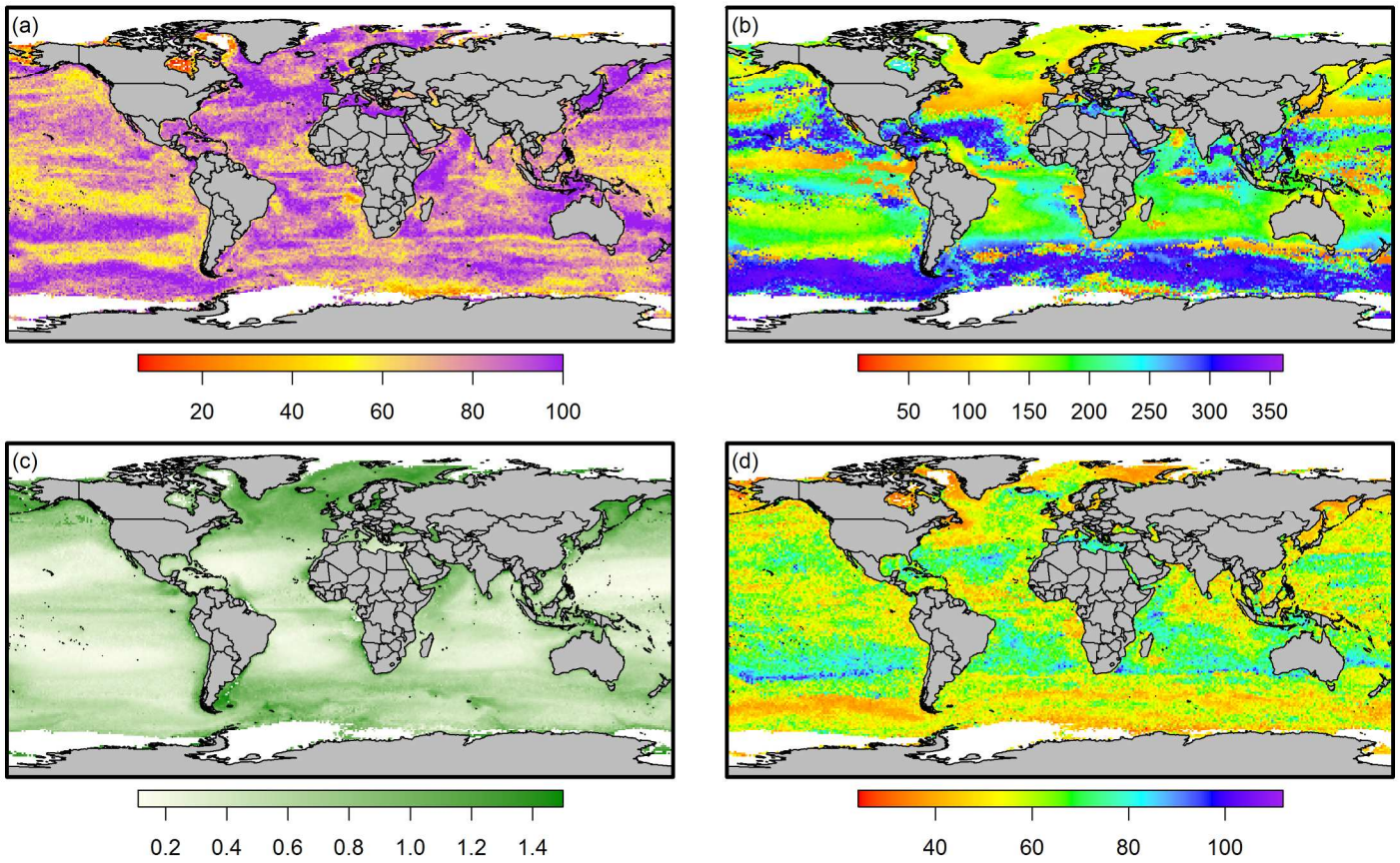

Figure 3 Correlation between bloom start day and duration (a), magnitude (b), and intensity (c) for the dominant annual bloom based on a global 1° latitudinal/longitudinal grid over the study period 1998-2015. Only grid locations with at least eight years with detected blooms were included; red makers indicate significant negative correlations ($\rho<0.05$), blue makers indicate significant positive correlations, and beige markers indicate non-significant correlations.

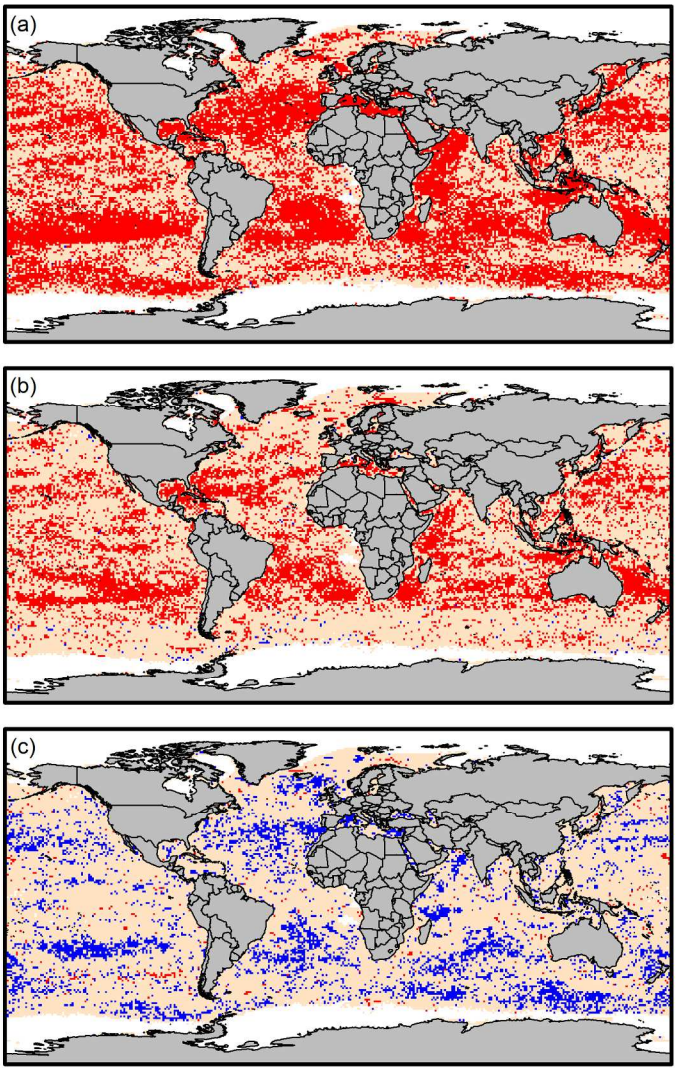

Figure 4 Relative Theil-Sen slope showing time series trends in start day (a), magnitude (b), intensity (c), and duration (d) for the dominant annual bloom based on a global 1° latitudinal/longitudinal grid over the study period 1998-2015. Only grid locations with at least ten years with detected blooms were included. Blue shades denote positive change and red denote negative change.

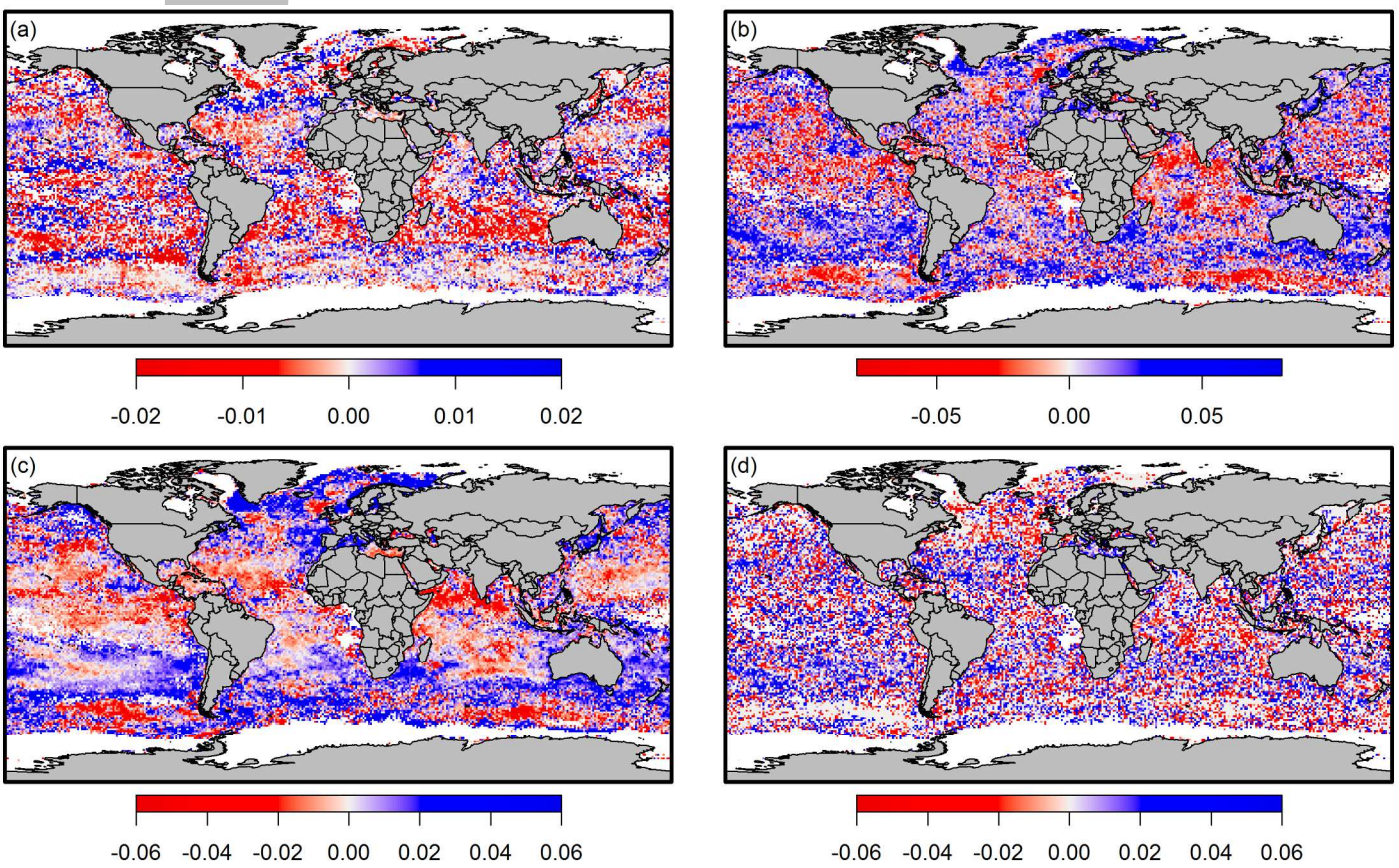

Figure 5 Mean annual relative Theil-Sen slope binned by 5° latitude and longitude groupings showing time series trends in start day (a and b, respectively), magnitude (c and d, respectively), intensity (e and f, respectively), and duration (g and h, respectively) for the dominant annual bloom based on a global 1° latitudinal/longitudinal grid over the study period 1998-2015. Only grid locations with at least ten years of detected blooms were included. Error bars are 95% confidence intervals and gray lines are LOESS smoothers using a span setting of 0.5.

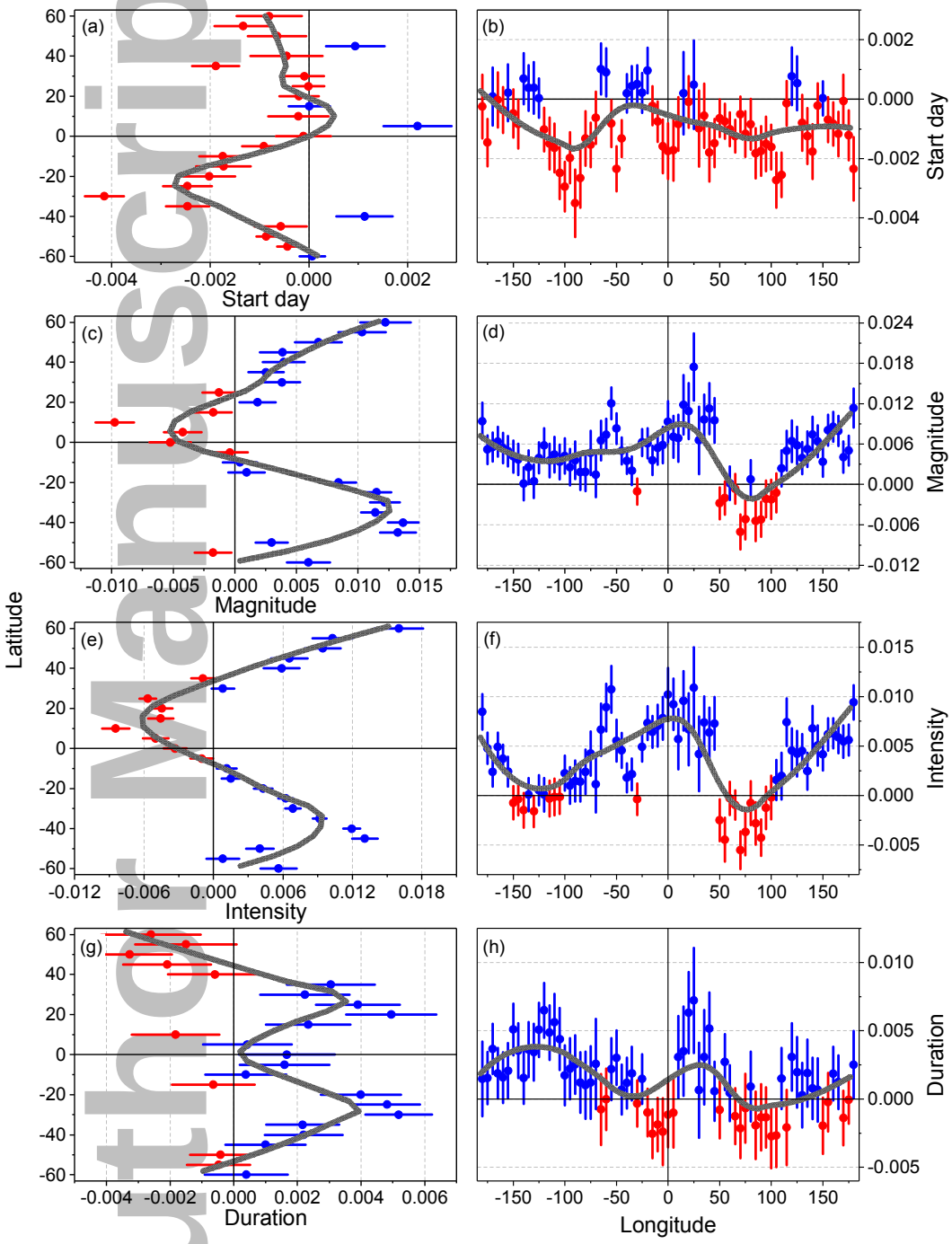

Figure 6. Relative Theil-Sen slope showing time series trends in sea surface temperature (a), salinity (b), mixed layer depth (c), zonal wind stress (d), and meridional wind stress (e) based on a global 1° latitudinal/longitudinal grid over the study period 1998-2015.

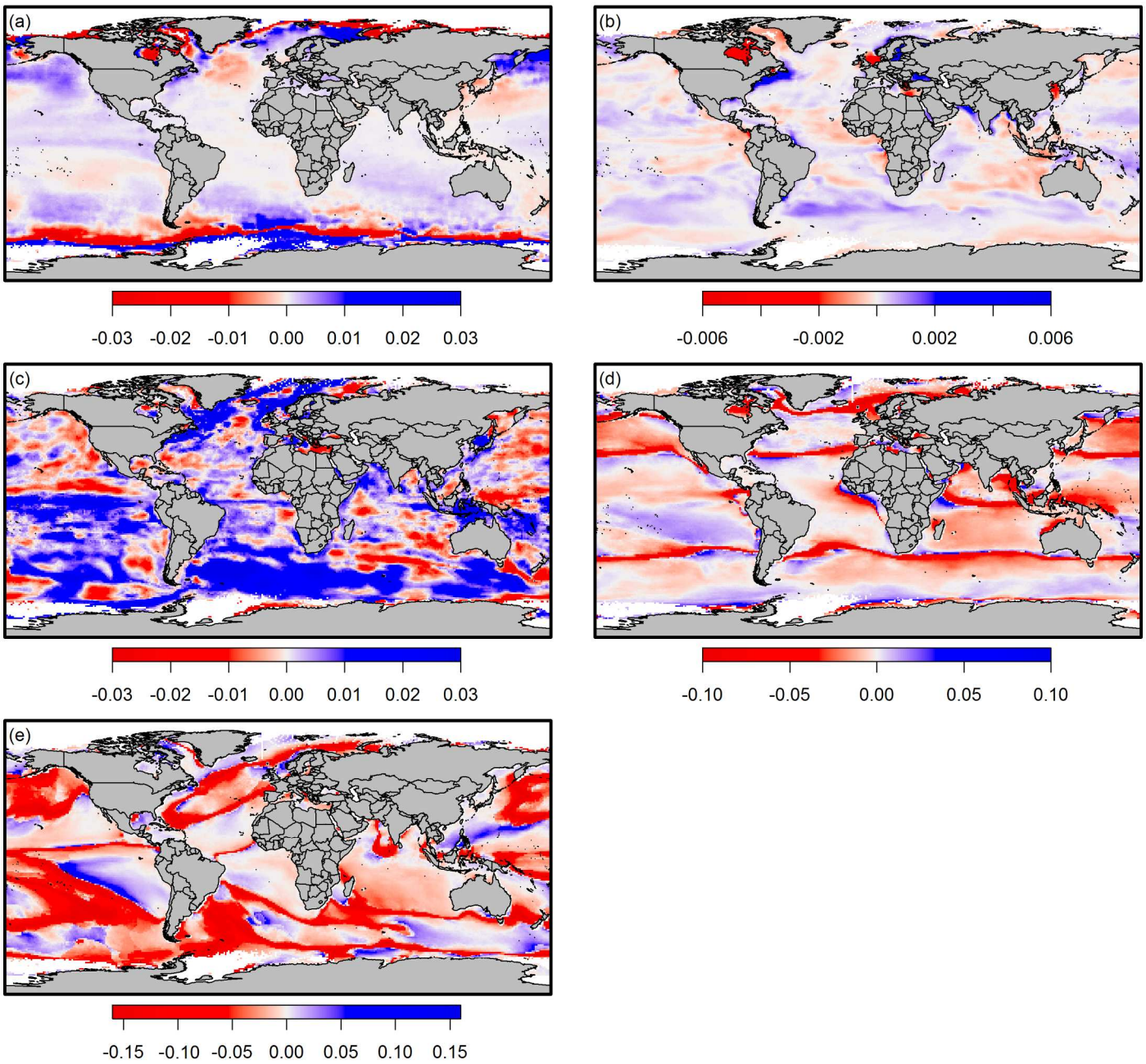

Figure 7. Mean annual relative Theil-Sen slope binned by 5° latitude and longitude groupings showing time series trends in SST (a and b, respectively), salinity (c and d, respectively), mixed layer depth (e and f, respectively), zonal wind stress (g and h, respectively), and meridional wind stress (i and j, respectively) for the dominant annual bloom based on a global 1° latitudinal/longitudinal grid over the study period 1998-2015. Only grid locations with at least ten years of detected blooms were included. Error bars are 95% confidence intervals and gray lines are LOESS smoothers using a span setting of 0.5.

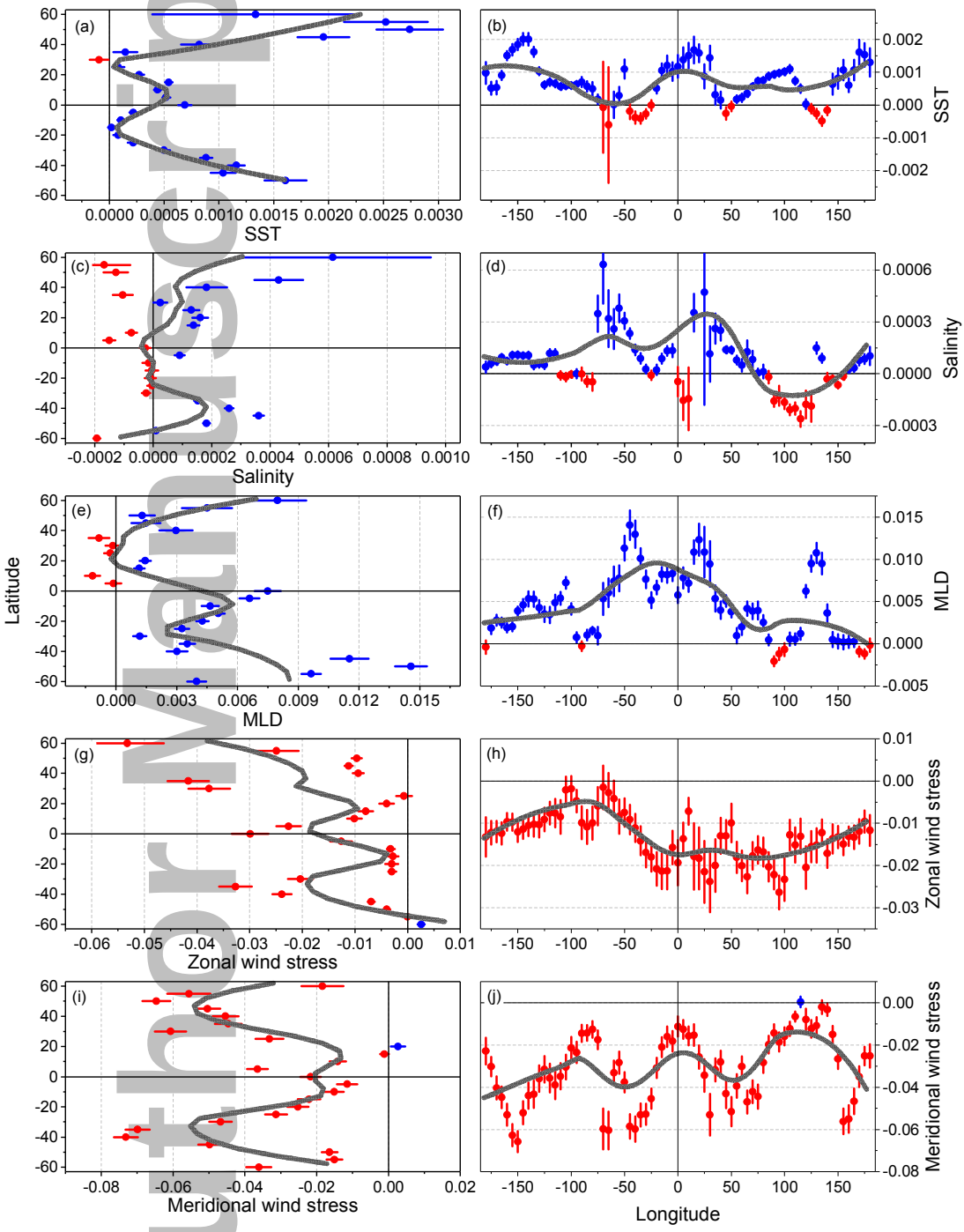

Figure 8 Mean global interval and cumulative absolute trends in bloom start day (a), magnitude (b), intensity (c), and duration (d) versus Mann-Kendall trend test probability intervals. Trends are the product of Theil-Sen slopes for the dominant annual bloom and the number of years in the time series. Probability interval 0.0 includes $p<0.05$, interval 0.1 includes $0.05 \leq p<0.15$, etc. Each interval estimate includes trends associated with that interval probability level only and are estimated from all data excluding outliers. Cumulative trends are based on data from the interval trends and all lower probability intervals. Only grid locations with at least ten years with detected blooms were included based on a global 1° latitudinal/longitudinal grid over the study period 1998-2015 excluding data from latitudes north and south of 62°N and 62°S, respectively. Error bar are 95% confidence intervals.

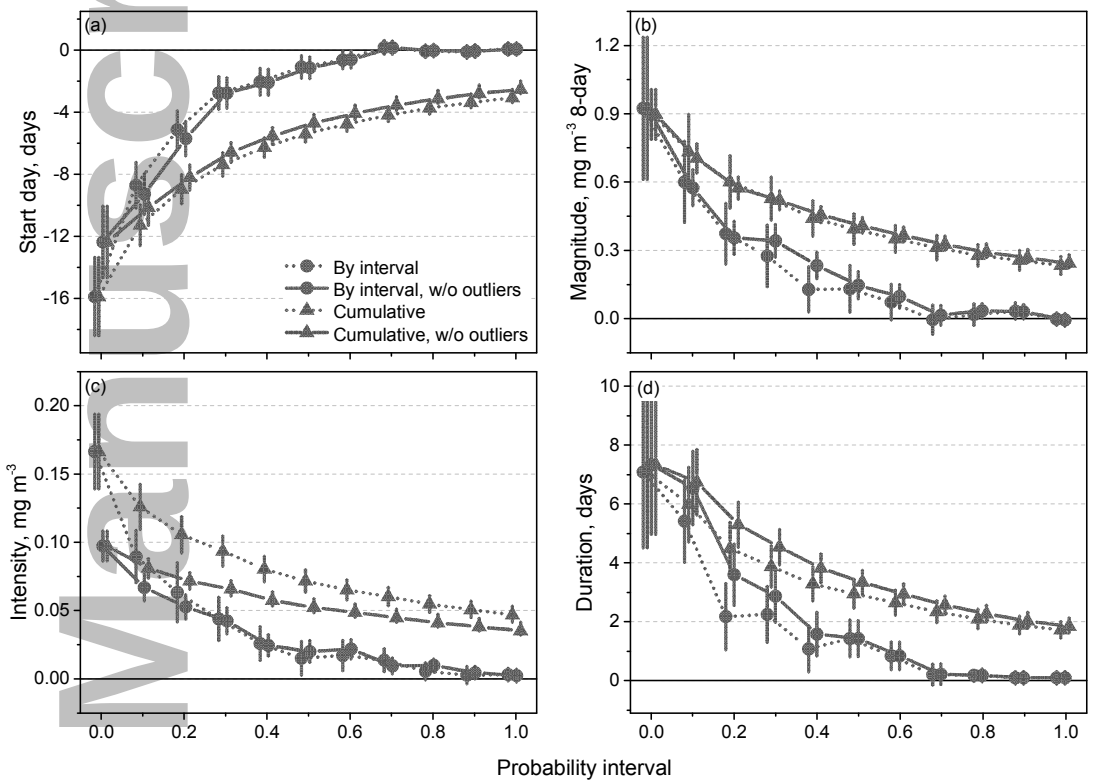

Figure 9 Mean absolute trends over ocean areas for bloom start day (a), magnitude (b), intensity (c), and duration (d) for areas regardless of significance level (all p-levels). Trends are the product of Theil-Sen slopes for the dominant annual bloom and the number of years in the times series based on a global 1° latitudinal/longitudinal grid over the study period 1998-2015 excluding data from latitudes north of 62°N and south of 62°S. Grid locations are combined as per ocean areas and oligotrophic versus non-oligotrophic area as per figure 1 [N_Atl, N_Pac = North Atlantic and Pacific (red circles); S_Atl, S_Ind, S_Pac = South Atlantic, Indian, and Pacific (green squares); T_Atl, T_Ind, T_Pac = Tropical Atlantic, Indian, and Pacific (blue triangles); Olig, Non-Olig = Oligotrophic and Non-Oligotrophic areas (magenta diamonds)]. Only grid locations with at least ten years with detected blooms were included and outliers were excluded. Error bar are 95% confidence intervals.

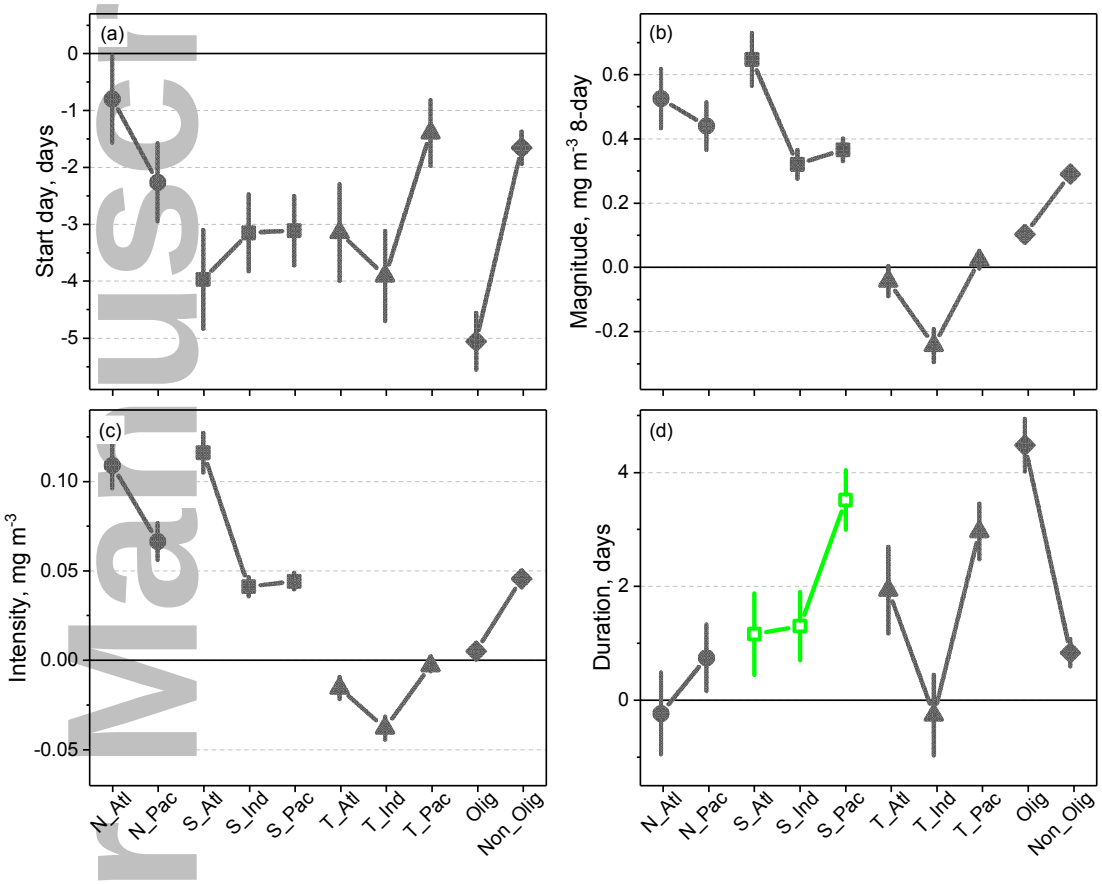

Figure 10 Mean absolute trends over ocean areas for bloom start day (a), magnitude (b), intensity (c), and duration (d) for areas with significant trends ($p<0.05$). Trends are the product of Theil-Sen slopes for the dominant annual bloom and the number of years in the times series based on a global 1° latitudinal/longitudinal grid over the study period 1998-2015 excluding data from latitudes north of 62°N and south of 62°S. Grid locations are combined as per ocean areas and oligotrophic versus non-oligotrophic area as per figure 1 [N_Atl, N_Pac = North Atlantic and Pacific (red circles); S_Atl, S_Ind, S_Pac = South Atlantic, Indian, and Pacific (green squares); T_Atl, T_Ind, T_Pac = Tropical Atlantic, Indian, and Pacific (blue triangles); Olig, Non-Olig = Oligotrophic and Non-Oligotrophic areas (magenta diamonds)]. Only grid locations with at least ten years with detected blooms were included and outliers were excluded. Error bar are 95% confidence intervals.

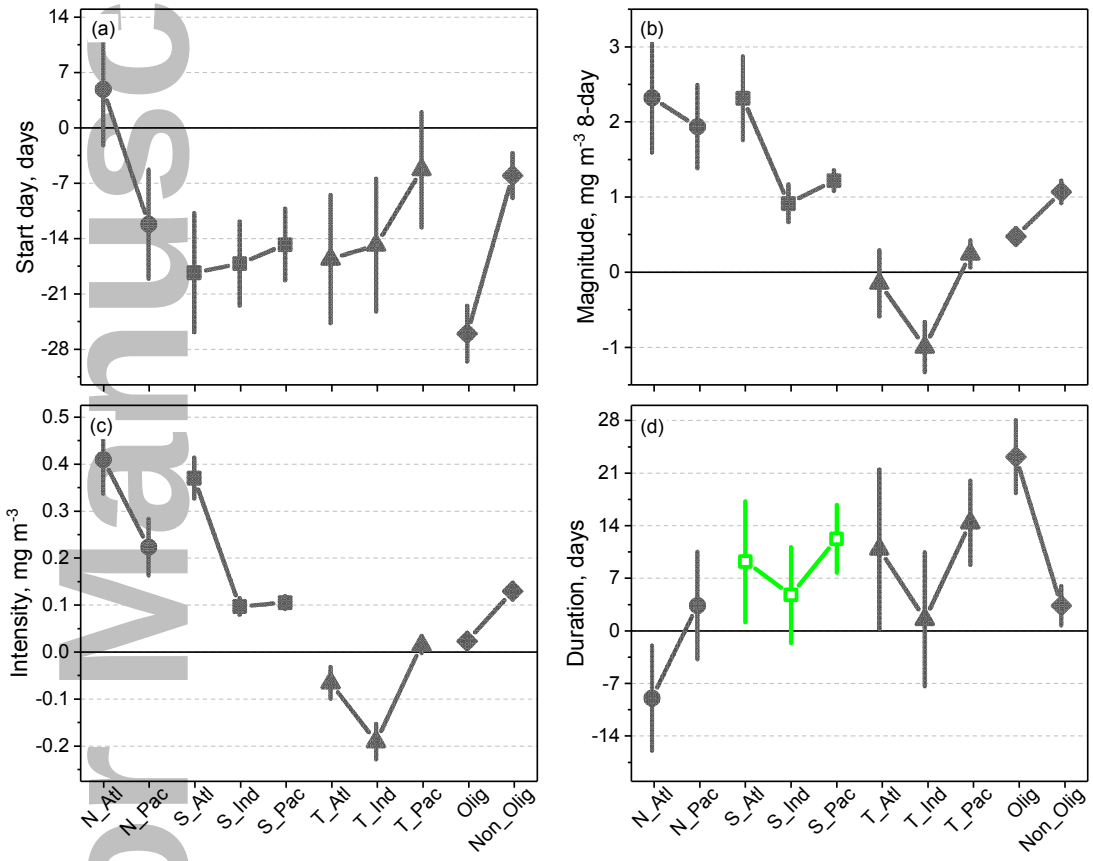

Short Title: Bloom intensity.

Appendix S1 Bloom intensity [log (mg m^{-3}+1)] for the dominant annual bloom based on a global 1° latitudinal/longitudinal grid over the study period 1998-2015.

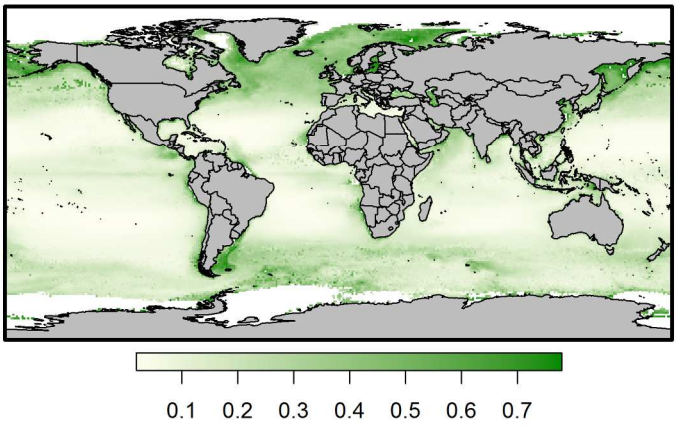

Supporting information **Appendix S2**

Short Title: Analysis of abiotic factors.

Figure s2-1. Correlation between monthly SST and bloom start day (a), duration (b), magnitude (c), and intensity (d) for the dominant annual bloom based on a global 1° latitudinal/longitudinal grid over the study period 1998-2015. Only grid locations with at least eight years with detected blooms were included; red makers indicate significant negative correlations (ρ<0.05), blue makers indicate significant positive correlations, and beige markers indicate non-significant correlations.

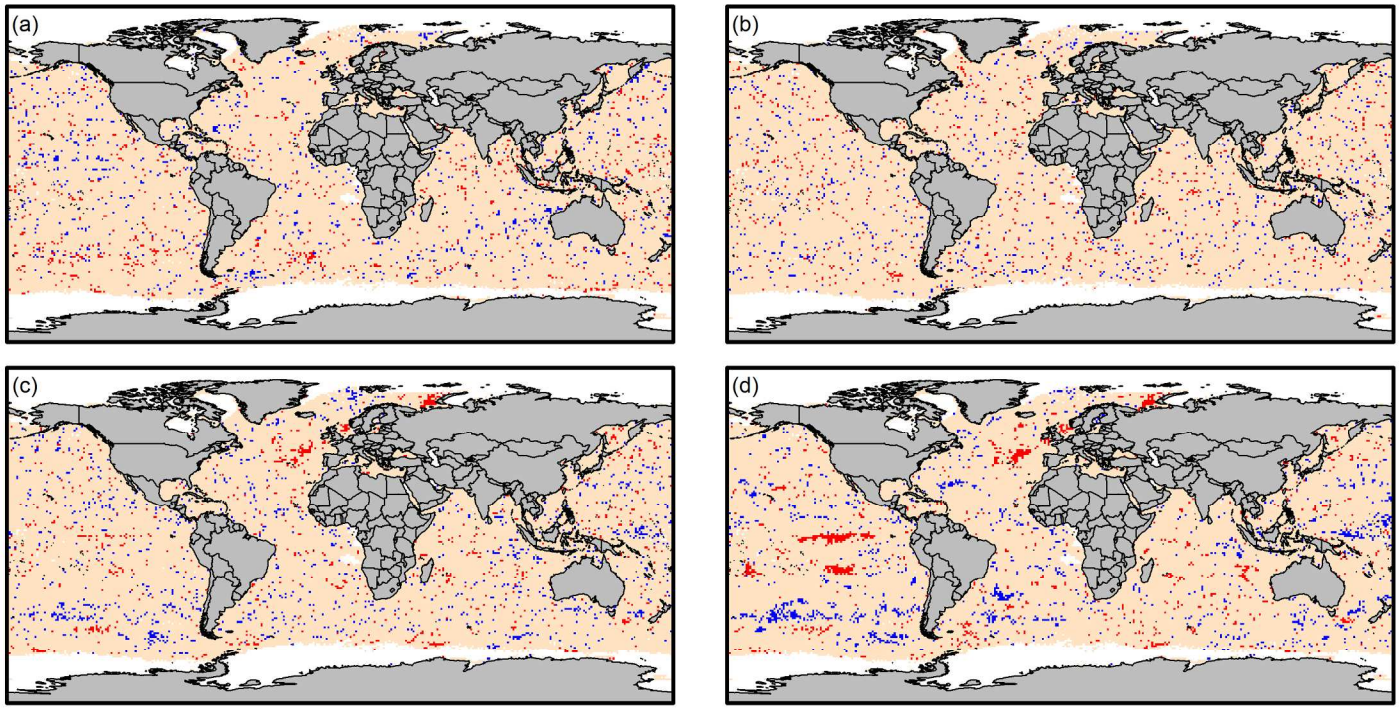

Figure s2-2. Correlation between annual mean SST and bloom start day (a), duration (b), magnitude (c), and intensity (d) for the dominant annual bloom based on a global 1° latitudinal/longitudinal grid over the study period 1998-2015. Only grid locations with at least eight years with detected blooms were included; red makers indicate significant negative correlations (ρ<0.05), blue makers indicate significant positive correlations, and beige markers indicate non-significant correlations.

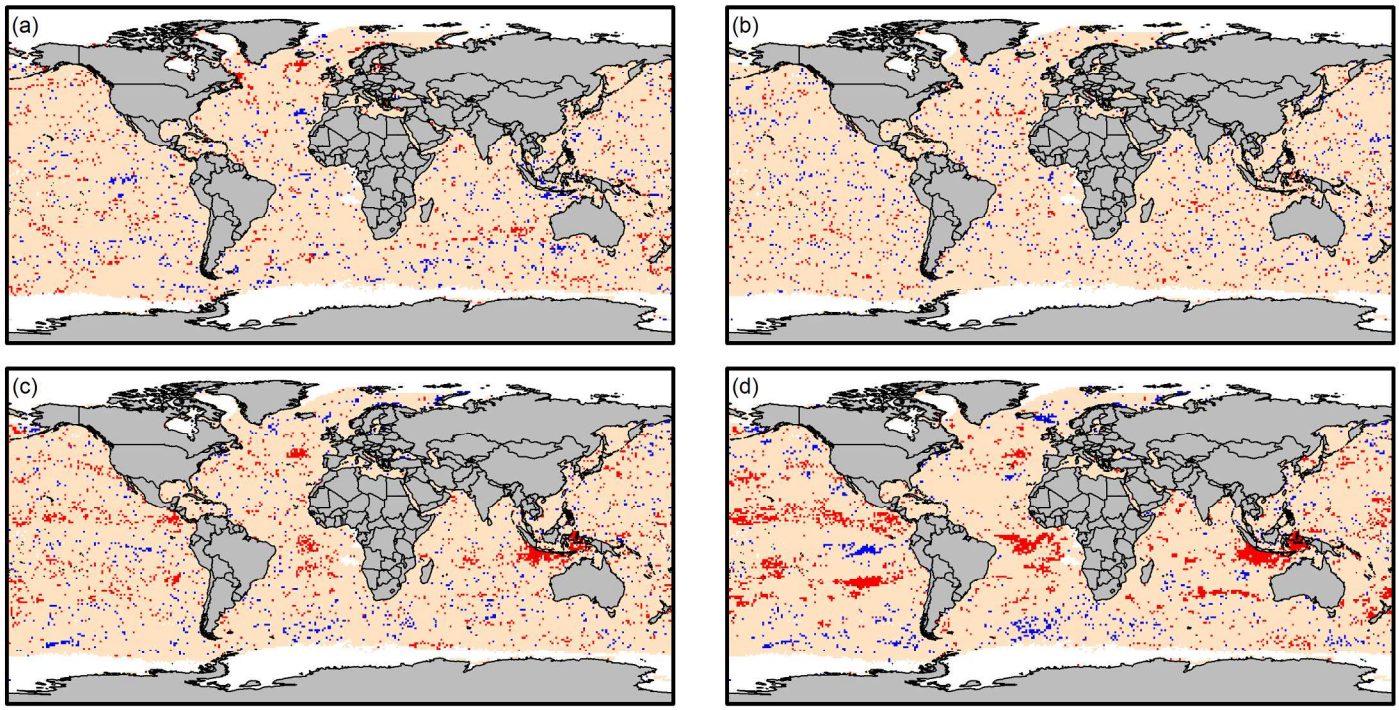

Figure s2-3. Correlation between monthly salinity and bloom start day (a), duration (b), magnitude (c), and intensity (d) for the dominant annual bloom based on a global 1° latitudinal/longitudinal grid over the study period 1998-2015. Only grid locations with at least eight years with detected blooms were included; red makers indicate significant negative correlations (ρ<0.05), blue makers indicate significant positive correlations, and beige markers indicate non-significant correlations.

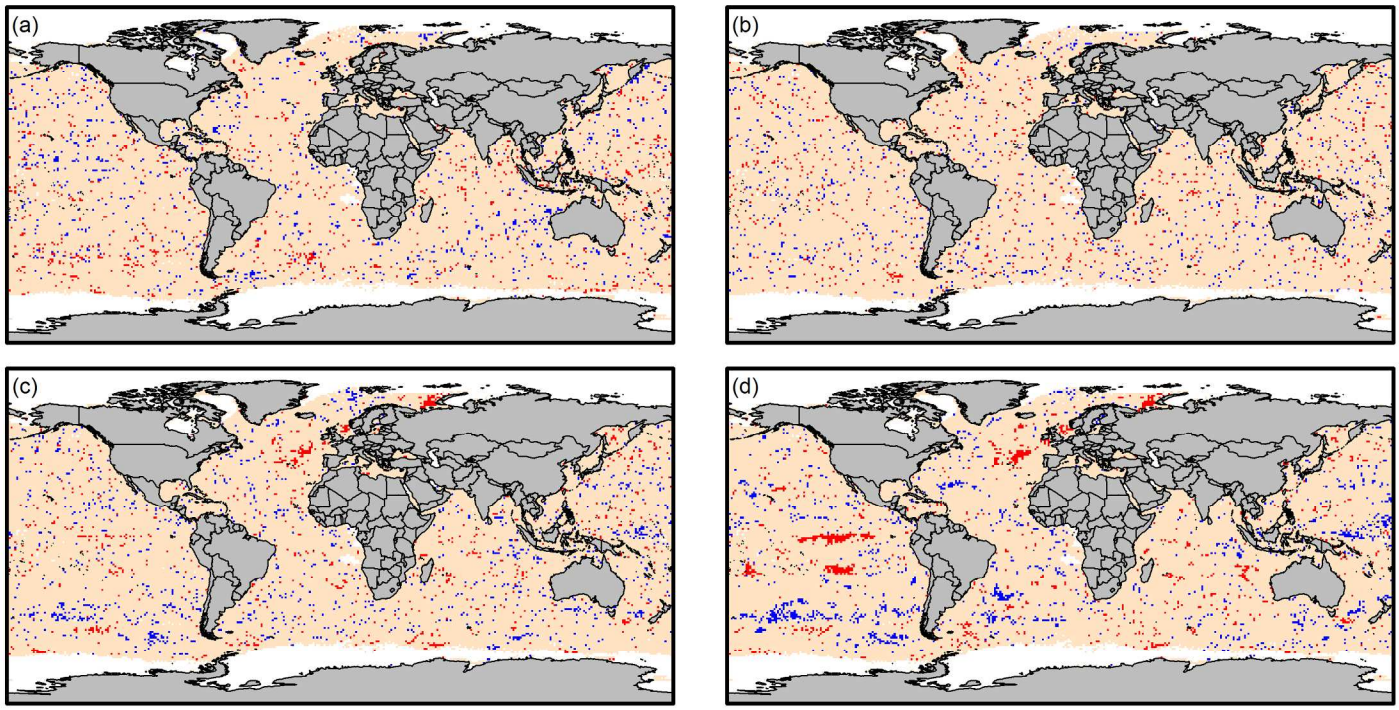

Figure s2-4. Correlation between mean annual salinity and bloom start day (a), duration (b), magnitude (c), and intensity (d) for the dominant annual bloom based on a global 1° latitudinal/longitudinal grid over the study period 1998-2015. Only grid locations with at least eight years with detected blooms were included; red makers indicate significant negative correlations (ρ<0.05), blue makers indicate significant positive correlations, and beige markers indicate non-significant correlations.

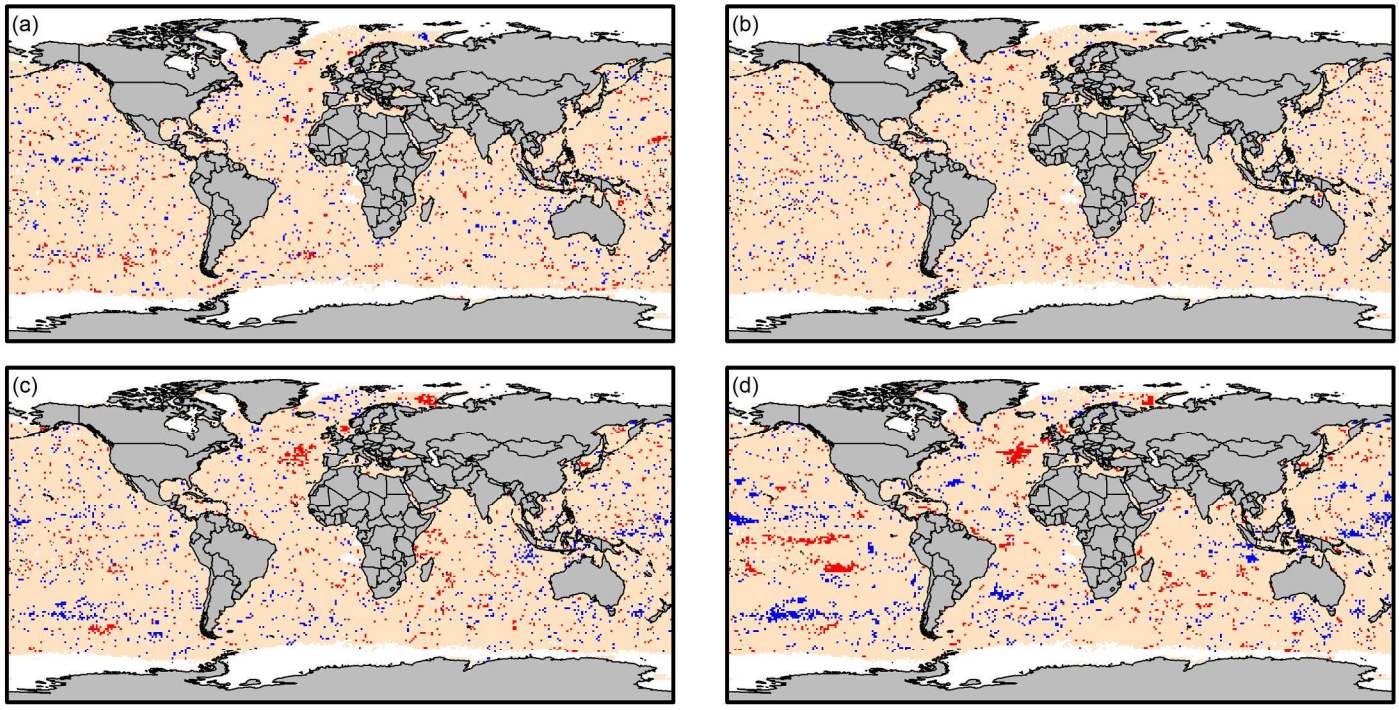

Figure s2-5. Correlation between monthly mixed layer depth and bloom start day (a), duration (b), magnitude (c), and intensity (d) for the dominant annual bloom based on a global 1° latitudinal/longitudinal grid over the study period 1998-2015. Only grid locations with at least eight years with detected blooms were included; red makers indicate significant negative correlations ($\rho<0.05$), blue makers indicate significant positive correlations, and beige markers indicate non-significant correlations.

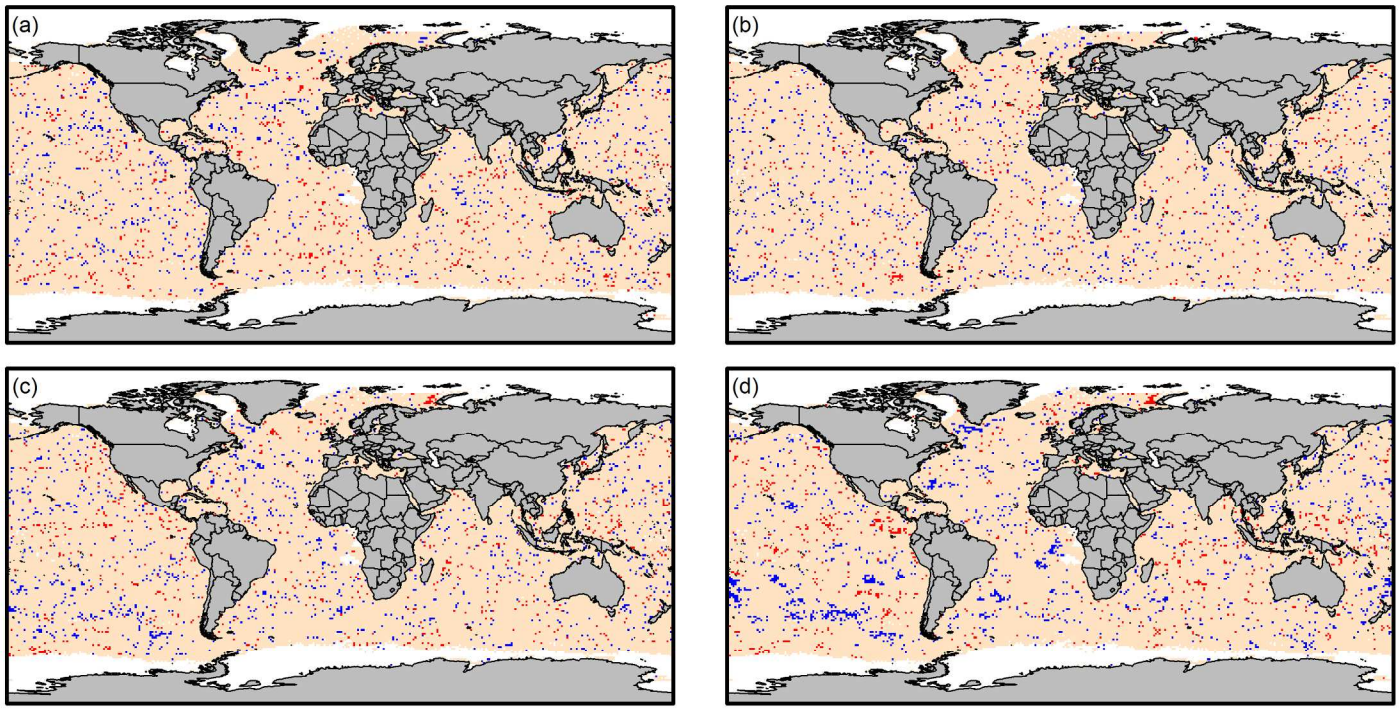

Figure s2-6. Correlation between mean annual mixed layer depth and bloom start day (a), duration (b), magnitude (c), and intensity (d) for the dominant annual bloom based on a global 1° latitudinal/longitudinal grid over the study period 1998-2015. Only grid locations with at least eight years with detected blooms were included; red makers indicate significant negative correlations ($\rho<0.05$), blue makers indicate significant positive correlations, and beige markers indicate non-significant correlations.

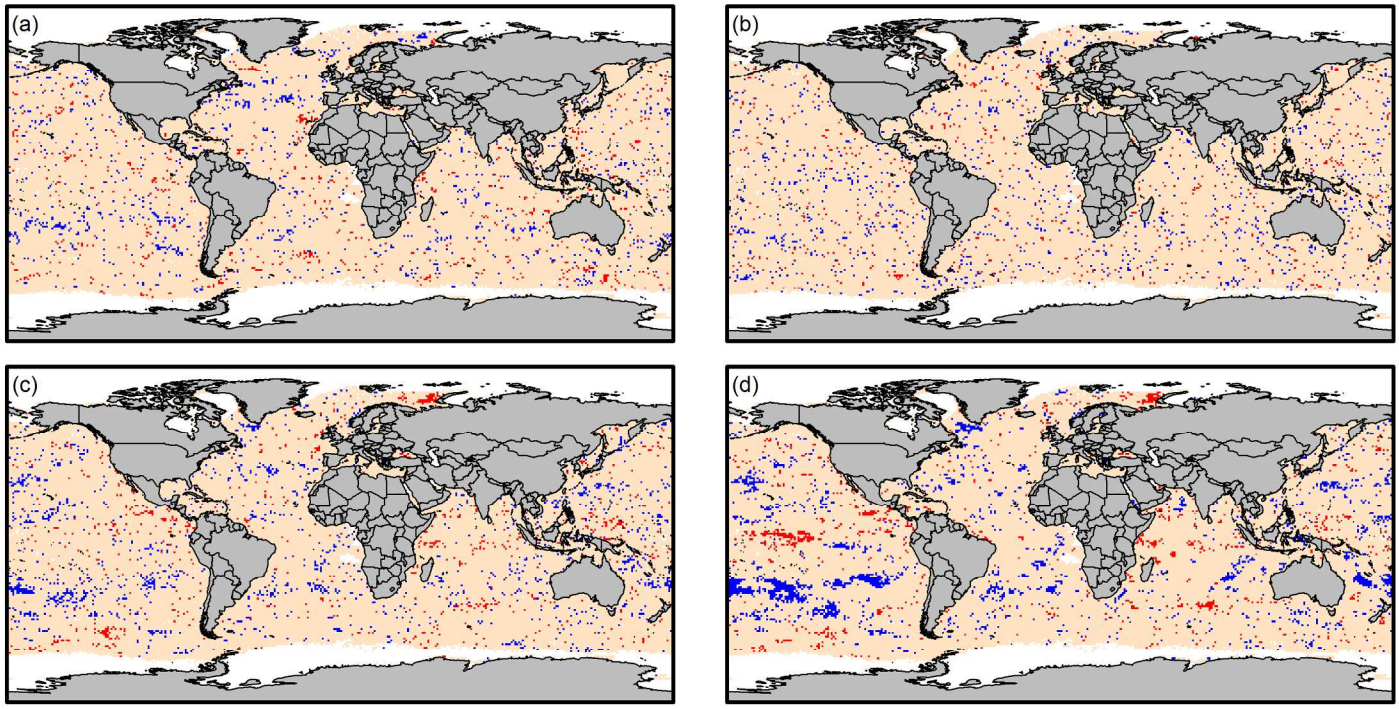

Figure s2-7. Correlation between monthly u-vector wind stress and bloom start day (a), duration (b), magnitude (c), and intensity (d) for the dominant annual bloom based on a global 1° latitudinal/longitudinal grid over the study period 1998-2015. Only grid locations with at least eight years with detected blooms were included; red makers indicate significant negative correlations ($\rho<0.05$), blue makers indicate significant positive correlations, and beige markers indicate non-significant correlations.

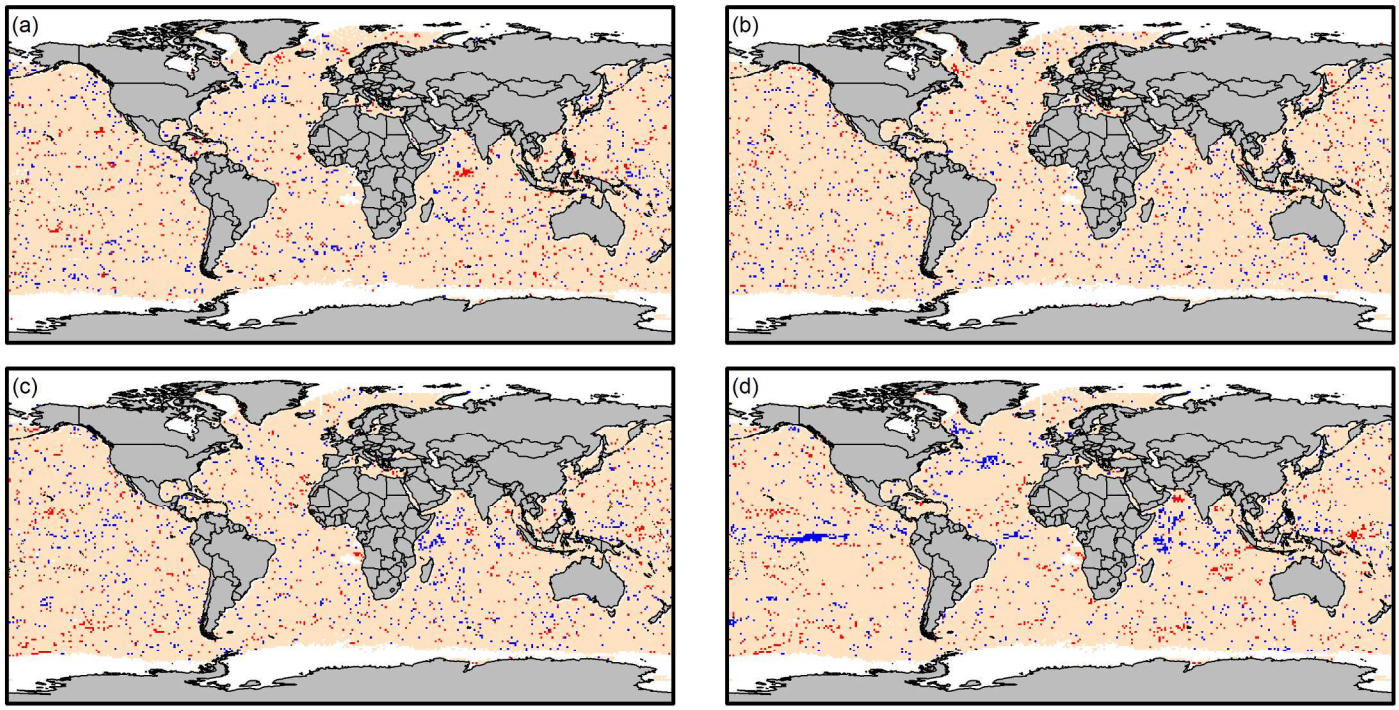

Figure s2-8. Correlation between mean annual u-vector wind stress and bloom start day (a), duration (b), magnitude (c), and intensity (d) for the dominant annual bloom based on a global 1° latitudinal/longitudinal grid over the study period 1998-2015. Only grid locations with at least eight years with detected blooms were included; red makers indicate significant negative correlations ($\rho<0.05$), blue makers indicate significant positive correlations, and beige markers indicate non-significant correlations.

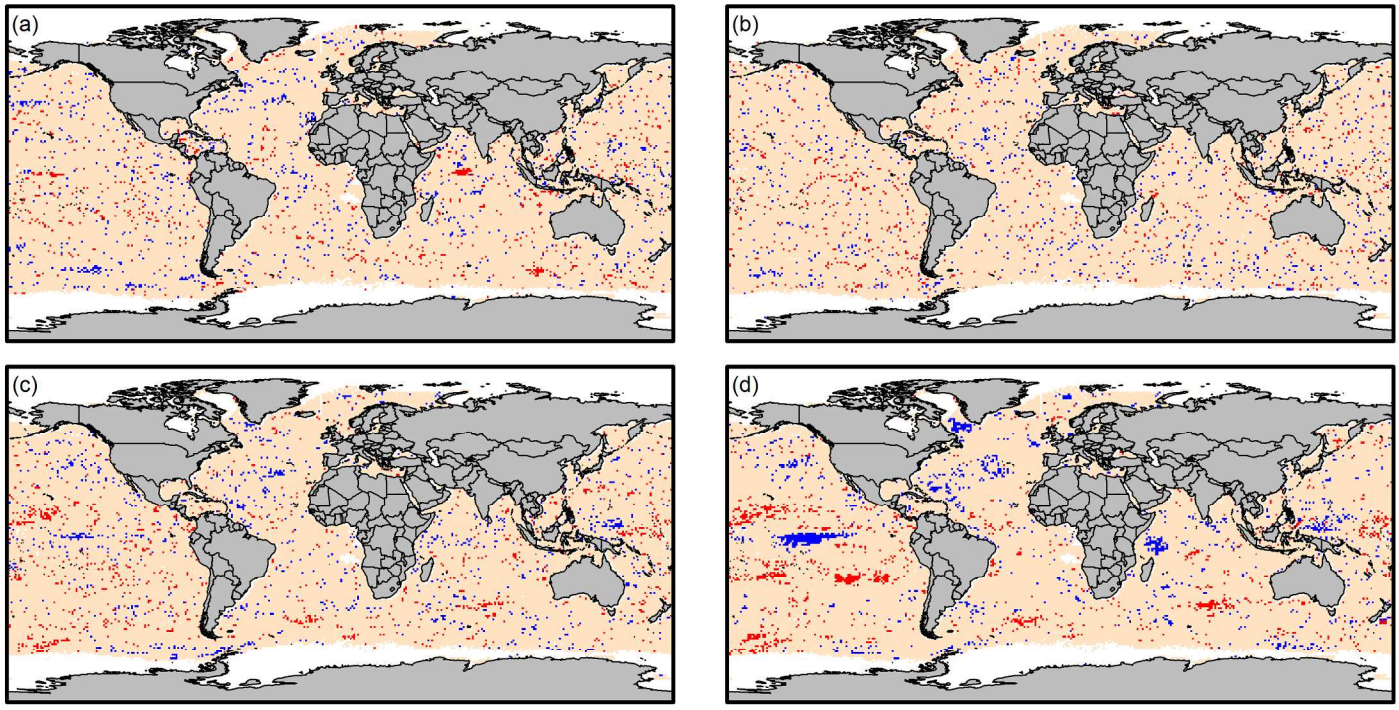

Figure s2-9. Correlation between monthly v-vector wind stress and bloom start day (a), duration (b), magnitude (c), and intensity (d) for the dominant annual bloom based on a global 1° latitudinal/longitudinal grid over the study period 1998-2015. Only grid locations with at least eight years with detected blooms were included; red makers indicate significant negative correlations ($\rho<0.05$), blue makers indicate significant positive correlations, and beige markers indicate non-significant correlations.

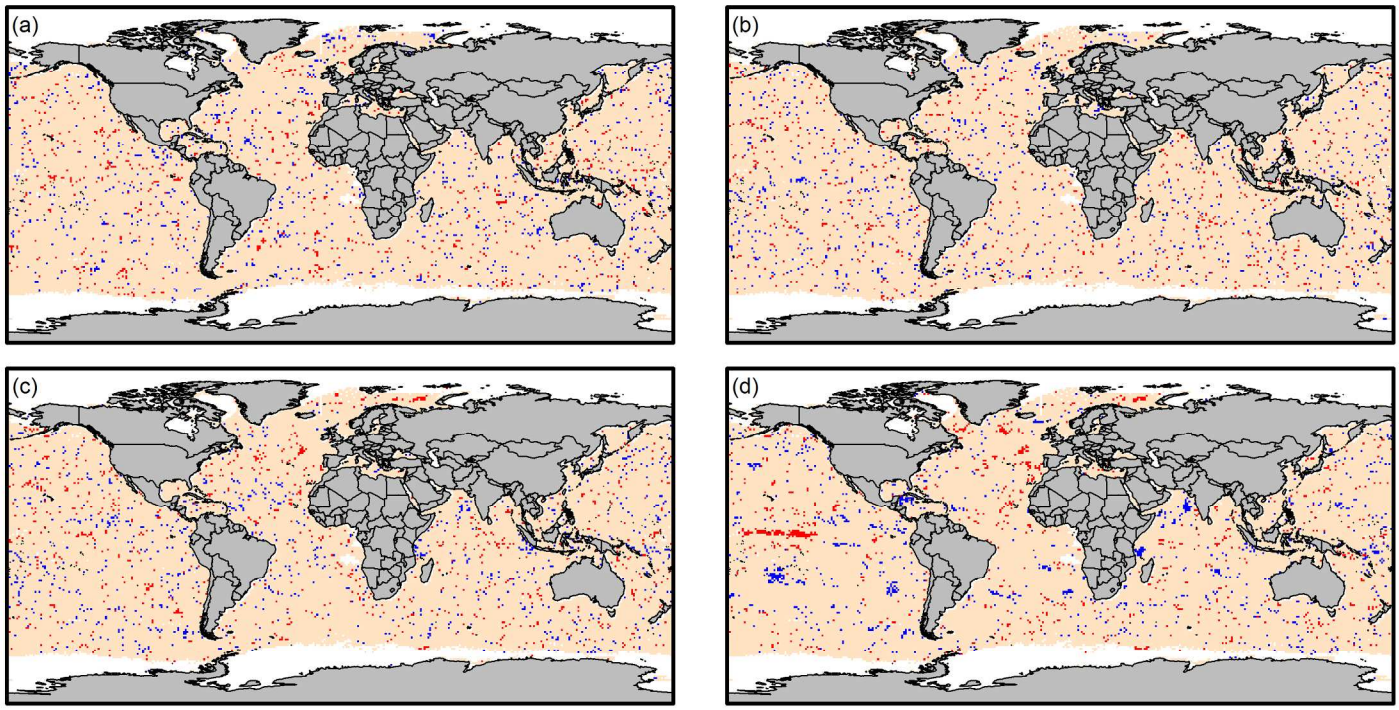

Figure s2-10. Correlation between mean annual v-vector wind stress and bloom start day (a), duration (b), magnitude (c), and intensity (d) for the dominant annual bloom based on a global 1° latitudinal/longitudinal grid over the study period 1998-2015. Only grid locations with at least eight years with detected blooms were included; red makers indicate significant negative correlations ($\rho<0.05$), blue makers indicate significant positive correlations, and beige markers indicate non-significant correlations.